Donnan Dialysis for Phosphate Recovery from Diverted Urine

Water Research

Revised: October 17, 2022

Stephanie N. McCartney[a], Hanqing Fan[a], Nobuyo Watanabe[b], Yuxuan Huang[a], and Ngai Yin Yip[*a,c]

[a] Department of Earth and Environmental Engineering, Columbia University, New York, New York 10027-6623, United States

[b] Department of Chemistry, Barnard College, New York, New York 10027-6598, United States

[c] Columbia Water Center, Columbia University, New York, New York 10027-6623, United States

[*] Corresponding author: Email: n.y.yip@columbia.edu, Phone: +1 212 8542984

Abstract

There is a critical need to shift from existing linear phosphorous management practices to a more sustainable circular P economy. Closing the nutrient loop can reduce our reliance on phosphate mining, which has well-documented environmental impacts, while simultaneously alleviating P pollution of aquatic environments from wastewater discharges that are not completely treated. The high orthophosphate, $H_xPO_4^{(3-x)-}$, content in source-separated urine offers propitious opportunities for P recovery. This study examines the use of Donnan dialysis (DD), an ion-exchange membrane-based process, for the recovery of orthophosphates from fresh and hydrolyzed urine matrixes. $H_2PO_4^-$ transport against an orthophosphate concentration gradient was demonstrated and orthophosphate recovery yields up to 93% were achieved. By adopting higher feed to receiver volume ratios, DD enriched orthophosphate in the product stream as high as ≈2.5× the initial urine feed concentration. However, flux, selectivity, and yield of orthophosphate recovery were detrimentally impacted by the presence of SO_4^{2-} and Cl^- in fresh urine, and the large amount of HCO_3^- rendered hydrolyzed urine practically unsuitable for P recovery using DD. The detrimental effects of sulfate ions can be mitigated by utilizing a monovalent ion permselective membrane, improving selectivity for $H_2PO_4^-$ transport over SO_4^{2-} by 3.1× relative to DD with a conventional membrane; but the enhancement was at the expense of reduced orthophosphate flux. Critically, widely available and low-cost/waste resources with sufficiently high Cl^- content, such as seawater and waste water softening regenerant rinse, can be employed to improve the economic viability of orthophosphate recovery. This study shows the promising potential of DD for P recovery and enrichment from source-separated urine.

Keywords: phosphorous, nutrient recovery, Donnan dialysis, urine, circular economy

1. Introduction

Global food security is indispensably dependent on the sufficient supply of bioavailable phosphate for fertilizers. The growing global population is projected to drive a ≈50−85% increase in phosphate fertilizer demand by 2050 (Mogollóna et al., 2018). At the same time, the prevailing practice for phosphorus (P) fertilizer production, phosphate rock mining, relies on finite and diminishing deposits (reserves are predicted to last only 50−100 years, with production projected to decline after 2033) (Elser and Bennett, 2011; Smil, 2000). Furthermore, phosphate rock mining and beneficiation require significant energy inputs of 0.80−1.66 kWh/kg-P (2002; Reta et al., 2018). In addition to the substantial energy required for industrial P production, downstream anthropogenic waste streams require further chemical and energy inputs for phosphate management (Bleiwas, 2011; Maurer et al., 2003; Schaubroeck et al., 2015). On average, a human excretes 820−1,200 mg-P daily, with 67% in urine and the remainder in feces (H. Jönsson, 2004; Karak and Bhattacharyya, 2011; Mihelcic et al., 2011). But due to the high costs, wastewater treatment plants (WWTPs) in the U.S. are not commonly equipped with advanced treatments dedicated to phosphorous removal (Larsen et al., 2009). Without adequate elimination at WWTPs, the nutrient is discharged into aquatic ecosystems, which results in eutrophication, harmful algal blooms, and hypoxic dead zones (Anderson et al., 2008; Conley et al., 2009; Diaz and Rosenberg, 2008; Michalak et al., 2013). These ecotoxic environments harm aquatic organisms and can pose public health threats from algal and cyanobacterial toxins in recreational waterbodies and drinking water supplies (Brooks et al., 2016; Hitzfeld et al., 2000). For these reasons, the biogeochemical flow of phosphate is flagged as exceeding the safe operating space for humanity and poses high risks under the planetary boundaries framework (Steffen et al., 2015). The current approach for P

58 management has clear shortcomings and a new paradigm that is more sustainable is urgently
59 needed (Guest et al., 2009; Li et al., 2015; Verstraete et al., 2009).

60 There has been considerable efforts to separate phosphorus from waste streams at WWTPs,
61 (Blackall et al., 2002; Larsen et al., 2007; Oehmen et al., 2007; Yeoman et al., 1988) but the focus
62 of most methods is P removal without capture. Such approaches can mitigate the downstream
63 environmental problems, but still operate as an inefficient take-make-dispose linear economy
64 model. Instead, orthophosphate, $H_xPO_4^{(3-x)-}$, can be simultaneously removed and recovered from
65 anthropogenic wastewaters within a circular economy model, specifically, phosphorous is
66 captured from wastewater and recycled back into the food chain (Commoner, 1971; McCartney et
67 al., 2020; Stahel, 2016; W. McDonough, 2002; Webster, 2015). Closing the nutrient loop can ease
68 the demand for phosphate mining to strengthen food security and alleviate P pollution of aquatic
69 environments, thereby represents a transformative evolution to a more sustainable approach for
70 phosphorous management.

71 The theoretical minimum energy for P recovery, governed by thermodynamic principles,
72 is substantially lower for the feed of source-separated urine (i.e., the liquid is diverted away from
73 black water and isolated) compared with other wastewaters (McCartney et al., 2021). For instance,
74 recovery of orthophosphate from urine is ≈13−34% less energy-intensive than treated wastewater
75 effluent (McCartney et al., 2021). This is because urine is rich in P (total orthophosphate, TOP =
76 $19-48\times10^{-3}$ mol/L), (Fittschen and Hahn, 1998; Larsen et al., 2013; Simha and Ganesapillai, 2017;
77 Udert et al., 2003a) whereas treated wastewater effluent is over 1−2 orders of magnitude more
78 dilute. There has been considerable efforts to study the recovery of orthophosphates from urine
79 and significant strides have been made, with the primary approach being mineral precipitation of
80 slow-release fertilizers, such as struvite and magnesium potassium phosphate (Liu et al., 2013;

Maurer et al., 2006; Rahman et al., 2014; Randall and Naidoo, 2018; Ronteltap et al., 2007b; Udert et al., 2003a; Udert et al., 2003b; Wang et al., 2005). However, the technique has potential risks for contamination by pharmaceuticals, endocrine disrupting compounds, and pathogens (Boer et al., 2018; Kemacheevakul et al., 2015; Lahr et al., 2016; Mullen et al., 2017; Ronteltap et al., 2007a; Tang et al., 2019). Alternatively, sorbents, e.g., metal (oxy)hydroxide, (Karageorgiou et al., 2007; Lu et al., 2013; Tanada et al., 2003; Xie et al., 2014; Zhang et al., 2009) can be used to separate orthophosphate from other constituents in urine. But sorbent regeneration is chemically costly and the technique is further disadvantaged by the unavoidable generation of waste brines that cannot be easily disposed (Maul et al., 2014).

Ion exchange membrane (IEM) processes offer viable options for orthophosphate separation from urine without being encumbered by the above limitations. Donnan dialysis (DD) using IEMs has demonstrated promising potential for orthophosphate separation from other wastewaters besides urine, achieving high recovery yields (up to 98.4%) (Chen et al., 2014; Shashvatt et al., 2021; Trifi et al., 2009). However, the previous studies examined orthophosphate recovery from solutions containing only orthophosphate anions, i.e., no other co-ions are included in the water chemistry (Chen et al., 2014; Shashvatt et al., 2021; Trifi et al., 2009). Actual waste streams, including urine, are complex water matrices with many anions, cations, and uncharged species. In particular, the ionic composition of urine is uniquely different from, say, raw sewage or treated secondary effluent, with significantly greater amounts of SO_4^{2-}, Cl^-, and HCO_3^-. Based on the general understanding of Donnan equilibrium theory, the presence of other anions in addition to orthophosphate is expected to have non-negligible and potentially detrimental effects on the process. In a past DD study, the presence of co-ions was shown to have deleterious impacts

on arsenate removal from groundwater, (Zhao et al., 2010) underscoring the need to better understand these effects to enable P recovery from urine using DD.

In this study, the performance of Donnan dialysis to drive the separation and recovery of orthophosphate from diverted human urine is assessed. First, the working principles of anion exchange membranes and Donnan dialysis are introduced. The exchange of $H_2PO_4^-$ and Cl^- across an anion-exchange membrane is then examined with DD experiments driven by the ion concentration gradients between an orthophosphate feed solution and a receiver solution of high chloride content. Next, the impact of receiver solution chloride concentration on P recovery is analyzed using simulated streams of brackish water, seawater, and desalination brine. The capability of DD to enrich orthophosphate in the receiver solution above the initial urine feed concentration is evaluated by adopting higher feed to receiver volume ratios. Then, the influence of other anions in urine on orthophosphate flux and recovery yield is studied, specifically, SO_4^{2-} and Cl^- in fresh urine, and SO_4^{2-}, Cl^-, and HCO_3^- in hydrolyzed urine. Enhancements in selectivity for orthophosphate transport over other anions using a monovalent ion permselective membrane are assessed and the potential of DD to harvest fertilizer products of aqueous orthophosphate solutions is investigated. Finally, implications of Donnan dialysis for P separation and recovery from urine are discussed.

2. Working Principles of Donnan Dialysis

2.1. Ion Exchange in Donnan Dialysis

In Donnan dialysis, DD, flux of driver ions down a concentration gradient, across an ion-exchange membrane (IEM), sets up an electrochemical potential to drive the transport of target ions in the opposite direction (Sarkar et al., 2010; Strathmann, 1995; Tanaka, 2015). IEMs are

polymeric thin-films with a high density of charged functional groups to allow the selective permeation of oppositely-charged counterions, while retaining like-charged co-ions (cation and anion exchange membranes, CEMs and AEMs, are selective for cation and anion transport, respectively) (Strathmann, 2004; Strathmann, 2010). The IEM separates the feed solution (FS) and receiver solution (RS). Driver counterions permeate from the higher concentration RS to the lower concentration FS. Because co-ions are rejected by the charge-selective membrane, target counterions in the FS migrate across the membrane in the opposite direction, into the RS, to preserve electroneutrality (Asante-Sackey et al., 2021; Chen et al., 2014; Hichour et al., 2000; Sarkar et al., 2010; Shashvatt et al., 2021; Velizarov, 2013; Yan et al., 2018). I.e., the electrochemical potential gradient across the IEM drives the exchange of counterions between the FS and RS in DD, with co-ions retained in the initial solutions (Sarkar et al., 2010). Note that the charge fluxes of driver and target ions must be equal to maintain electroneutrality. Importantly, an adequately large driver ion concentration difference across the membrane can enable migration of target ions against a concentration gradient, to achieve "uphill" transport (Tanaka, 2015).

In DD recovery of orthophosphates, $H_xPO_4^{(3-x)-}$, an AEM is employed to exchange $H_xPO_4^{(3-x)-}$ target ions from the FS with driver anions in the RS (Chen et al., 2014; Shashvatt et al., 2021; Trifi et al., 2009). Chloride is a suitable driver ion because Cl^- is present in high concentrations in low-cost or waste streams that are widely available, such as brackish water, seawater, desalination brine, and waste effluent from water softening regeneration. Critically, Cl^- concentrations in these streams are significantly higher than in urine ($>200\times10^{-3}$ mol/L, compared to $\approx100\times10^{-3}$ mol/L), to establish a sufficiently large electrochemical potential gradient across the AEM for uphill transport of $H_xPO_4^{(3-x)-}$. Therefore, this study will investigate DD recovery of orthophosphates using chloride as the RS driver counterion. Figure 1 depicts the DD separation of

148 orthophosphates from other constituents in urine feed solution and capture in the chloride-rich
149 receiver solution: $H_xPO_4^{(3-x)-}$ in the FS exchanges with Cl^- in the RS across the AEM, while
150 cations, M^+, are rejected by the charge-selective membrane. Note that one $H_xPO_4^{(3-x)-}$ ion
151 exchanges with (3−x) Cl^- ion(s) to maintain electroneutrality.

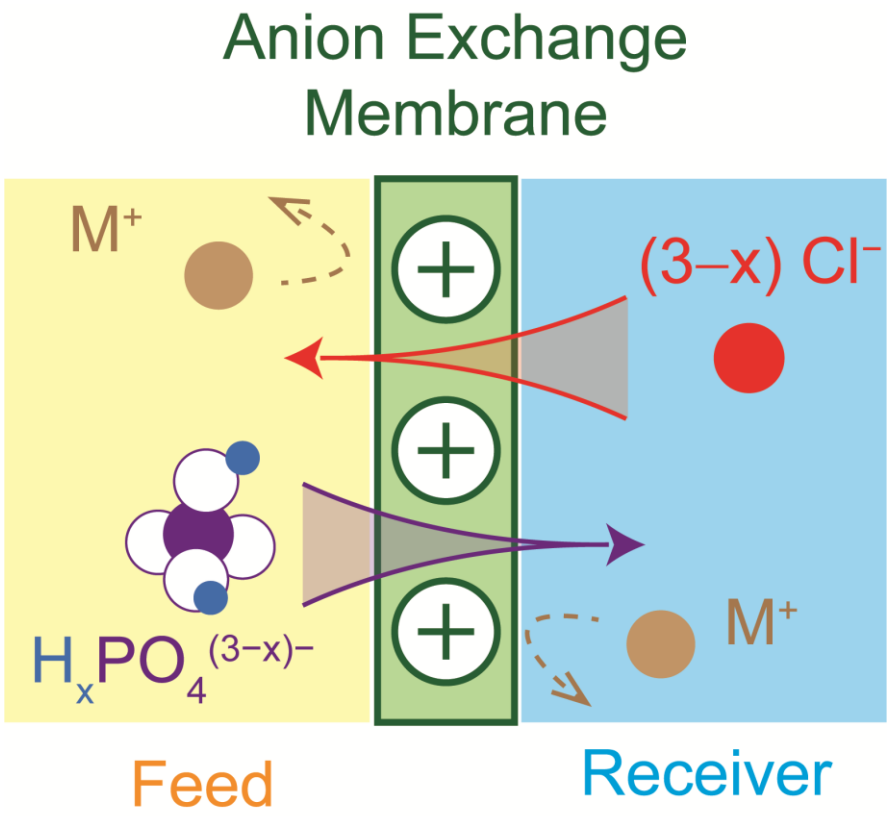

152
153 **Figure 1.** Schematic depicting Donnan dialysis recovery of orthophosphates. Exchange of counterions
154 (anions) across an anion exchange membrane (AEM) is driven by an electrochemical potential gradient
155 across the membrane, while co-ions (cations, M^+) are rejected by the charge-selective membrane and
156 retained in initial solutions. Driver ions, Cl^-, transport down a concentration gradient from the high
157 concentration RS to low concentration FS. The positively-charged AEM excludes M^+ cations. Therefore,
158 to maintain electroneutrality, target ions, $H_xPO_4^{(3-x)-}$, transport in the opposite direction, i.e., from FS
159 to RS. The charge fluxes of driver and target ions must be equal to maintain electroneutrality, i.e.,
160 $H_xPO_4^{(3-x)-}$ exchanges with (3−x) Cl^- ions.

2.2. Orthophosphate Recovery at Donnan Equilibrium

Target and driver counterions in the FS and RS exchange until Donnan equilibrium is reached, i.e., electrochemical potential gradient across the membrane = 0. For the system with $H_xPO_4^{(3-x)-}$ and Cl^- as target and driver ions, respectively, concentrations in the FS and RS at Donnan equilibrium are governed by eq 1 (derivation is detailed in eqs S1–4 of the Supplementary Material):

$$\frac{\left[H_xPO_4^{(3-x)-}\right]_{FS,f}}{\left[H_xPO_4^{(3-x)-}\right]_{RS,f}} \approx \left(\frac{\left[Cl^-\right]_{FS,f}}{\left[Cl^-\right]_{RS,f}}\right)^{(3-x)} \quad (1)$$

where subscripts FS and RS denote feed and receiver solutions, respectively, and *f* signifies final equilibrium. Note that eq 1 assumes perfect cation rejection and negligible water transport across the AEM.

To determine final target and driver ion concentrations at Donnan equilibrium using known initial concentrations, the principles of electroneutrality and material balances can be applied and are represented by eqs S5–8 of the Supplementary Material. For equivalent FS and RS volumes (i.e., $V_{FS} = V_{RS}$), $H_xPO_4^{(3-x)-}$ as the sole initial anion in the FS, and Cl^- as the sole initial anion in the RS, eq 2 describes the relationship between initial concentrations and final concentrations at Donnan equilibrium:

$$\frac{\left[H_xPO_4^{(3-x)-}\right]_{FS,0} - \left[H_xPO_4^{(3-x)-}\right]_{RS,f}}{\left[H_xPO_4^{(3-x)-}\right]_{RS,f}} \approx \left(\frac{(3-x)\left[H_xPO_4^{(3-x)-}\right]_{RS,f}}{\left[Cl^-\right]_{RS,0} - (3-x)\left[H_xPO_4^{(3-x)-}\right]_{RS,f}}\right)^{(3-x)} \quad (2)$$

$[H_xPO_4^{(3-x)-}]_{RS,f}$ can be determined using initial concentrations $[H_xPO_4^{(3-x)-}]_{RS,0}$ and $[Cl^-]_{FS,0}$. The moles of orthophosphate recovered is the product of concentration and volume of

the final RS solution, $[H_xPO_4^{(3-x)-}]_{RS,f}V_{RS}$. Eqs S9–17 of the Supplementary Material are the Donnan equilibrium expressions for systems with different initial conditions, specifically multiple anions in the FS ($H_xPO_4^{(3-x)-}$, SO_4^{2-}, and Cl^-) and non-equivolume scenarios ($V_{FS} \neq V_{RS}$).

3. Materials and methods

3.1. Materials and chemicals

Commercial anion exchange membranes of Selemion AMV and Selemion ASVN, a monovalent ion-selective AEM, were procured from Asahi Glass Co. (Japan). Four DD cells with different chamber volumes were fabricated using Mars Pro MSLA 3D Printer acquired from Elegoo (China). The solutions in each chamber were constantly stirred using magnetic stirring bars. The feed and receiver chamber volumes, respectively, are: 20 and 20 mL; 40 and 20 mL; 80 and 20 mL; and 40 and 40 mL, for feed to receiver solution volume ratios of 1:1, 2:1, 4:1, and 2:2, respectively. The effective membrane areas in all cells are 9.0 cm^2. $Na_2HPO_4 \cdot 7H_2O$, $Na_3PO_4 \cdot 12H_2O$, NaCl, $MgCl_2 \cdot 6H_2O$, $MgSO_4 \cdot 7H_2O$, and NH_4Cl salts were obtained from Alfa Aesar (Ward Hill, MA). KCl salt, 85% H_3PO_4 solution, and 2.5 M H_2SO_4 were acquired from Lab Chem (Zelienople, PA), Fisher Scientific (Waltham, MA), and Titripur (St. Louis, MO), respectively. All chemicals are ACS grade and were used as received. All solutions were prepared using deionized (DI) water from a Milli-Q ultrapure water purification system (Millipore Co., Burlington, MA).

3.2. Orthophosphate and Chloride Exchange in Donnan Dialysis

To demonstrate the exchange of $H_2PO_4^-$ in a feed solution, FS, with Cl^- in a receiver solution, RS, DD experiments were conducted with 30×10^{-3} mol/L $H_2PO_4^-$ initial FS (16.5×10^{-3}

mol/L $Na_2HPO_4 \cdot 7H_2O$ and 13.5×10^{-3} mol/L H_3PO_4; pH = 6.0) and 600×10^{-3} mol/L Cl^- (as NaCl) initial RS. The 20:20 mL cell was utilized. $H_2PO_4^-$ concentrations in the FS and RS and Cl^- concentrations in the RS were measured at 1.0 h intervals for 6.0 h. 175 µL samples were collected from each solution and the anion concentrations were analyzed using ion chromatography, IC (Dionex Aquion, Thermo Fisher Scientific, Waltham, MA).

3.3. Characterization of Orthophosphate Recovery at Donnan Equilibrium

Orthophosphate, sulfate, and bicarbonate transport from FS to RS and chloride transport from RS to FS were evaluated in different DD operations. Three FS were utilized in orthophosphate recovery experiments: i. feed solution with the total orthophosphate, TOP, concentration and pH of fresh urine, (Fittschen and Hahn, 1998; Larsen et al., 2013; Simha and Ganesapillai, 2017; Udert et al., 2003a) but without other anions (16.5×10^{-3} mol/L $Na_2HPO_4 \cdot 7H_2O$ and 13.5×10^{-3} mol/L H_3PO_4; pH = 6.0), ii. simulated fresh urine with the TOP, sulfate, and chloride concentrations, and pH of actual fresh urine (Fittschen and Hahn, 1998; Larsen et al., 2013; Simha and Ganesapillai, 2017; Udert et al., 2003a) (24×10^{-3} mol/L $Na_2HPO_4 \cdot 7H_2O$, 6×10^{-3} mol/L $Na_3PO_4 \cdot 12H_2O$, 100×10^{-3} mol/L NaCl, and 16×10^{-3} mol/L H_2SO_4), and iii. simulated hydrolyzed urine with the TOP, sulfate, chloride, and bicarbonate concentrations, and pH of actual hydrolyzed urine (Fittschen and Hahn, 1998; Udert et al., 2003a) (30×10^{-3} mol/L $Na_2HPO_4 \cdot 7H_2O$, 100×10^{-3} mol/L NaCl, 144×10^{-3} mol/L Na_2CO_3, and 106×10^{-3} mol/L $NaHCO_3$), as presented in Table 1. All solutions simulated the TOP concentration of undiluted urine (i.e., not mixed with flush water). Note that hydrolyzed urine is formed when urea, $CO(NH_2)_2$, in urine hydrolyses to form ammoniacal nitrogen and bicarbonate, which in turn increases the pH from ≈6.0 to ≈9.2 (Udert et al., 2003a; Udert et al., 2003b). At those pHs, the predominant orthophosphate species in simulated fresh and hydrolyzed urine solutions are $H_2PO_4^-$ and HPO_4^{2-}, respectively. Three receiver

solutions with NaCl concentrations of 200×10^{-3} mol/L, 600×10^{-3} mol/L, and $1{,}000\times10^{-3}$ mol/L were utilized to simulate brackish water, seawater, and seawater desalination brine, respectively. DD cells with feed chamber volumes of 20, 40, and 80 mL were employed for orthophosphate recovery experiments with different feed to receiver solution volume ratios. In summary, FS anion composition and RS Cl^- concentration were the parameters assessed in different FS to RS volume ratios. Unless stated otherwise, AMV membranes were used in the experiments. Pressure and temperature were at ambient conditions in all experiments.

Table 1. Anion compositions and pHs of feed solution containing only orthophosphate, simulated fresh urine, and simulated hydrolyzed urine.

Simulated Feed Solution	Ion Concentration ($\times10^{-3}$ mol/L)				pH
	$[H_xPO_4^{(3-x)-}]$	$[SO_4^{2-}]$	$[Cl^-]$	$[HCO_3^-]$	
TOP-only	30	0	0	0	6.0
Fresh urine	30	16	100	0	6.0
Hydrolyzed urine	30	16	100	250	9.2

Total orthophosphate, sulfate, and bicarbonate concentrations in the FS and RS, and chloride concentration in the FS were sampled and analyzed using ion chromatography. The measurement intervals were 12, 24, or 48 h for experiments with FS to RS volume ratios of 1, 2, and 4, respectively, with longer time allotted for experiments with higher ratios to approach equilibrium. The experiments were considered to have effectively equilibrated when the moles of exchanged orthophosphate ions remained consistent over three consecutive measurements (< 5% change); experimental duration is < ≈300 h for the longest run (FS to RS volume ratio of 4). Note that the sampling times are relatively long because the solution volumes are large compared to the effective membrane area. Additionally, the equilibration is asymptotic and, hence, the ions

exchange rates slow significantly as the process approaches equilibrium. Water transport was assessed by measuring feed and receiver solution volumes at the end of each experiment. Recovery yield, Y, is defined as the moles of TOP in the final RS normalized by the moles in the initial FS.

3.4. Evaluation of Anion Transport Kinetics

Anion fluxes from FS to RS were examined in DD kinetic experiments, i.e., final Donnan equilibriums were not reached in the tests. Fluxes were determined from the rate of change of anion concentrations in the RS over 2.0 and 8.0 h for the AMV and ASVN membranes, respectively. The sampling durations were selected for sufficient ions to permeate across the small membrane areas of the benchscale setup such that the solution concentrations were above detection limits of the IC (the ASVN experiments required more time because anion fluxes are relatively lower). Water transport across the AEMs during the kinetic experiments was not observed and deemed to be practically negligible. The change in moles of anion in the RS over time normalized by the membrane area yields flux, J_i. Flux selectivity, J_i/J_T, is defined as J_i normalized by the sum of all anion fluxes from feed to receiver solution.

Anion fluxes and flux selectivities were assessed for the AMV membrane using 600×10^{-3} mol/L NaCl RS with the three FS of TOP-only solution, simulated fresh urine, and simulated hydrolyzed urine. J_i and J_i/J_T were determined for the ASVN membrane using simulated fresh and hydrolyzed urine as FS and RS of 600×10^{-3} mol/L NaCl. To demonstrate the potential of DD to recover orthophosphate and yield aqueous products, experiments were conducted using the ASVN membrane, simulated fresh urine as FS, and four different RS. The RS investigated are: i. 600×10^{-3} mol/L NaCl, ii. 600×10^{-3} mol/L KCl to simulate aqueous potash fertilizer, iii. waste water softening regenerant rinse, WWSRR (547×10^{-3} mol/L KCl and 48×10^{-3} mol/L $MgCl_2\cdot6H_2O$), iv. and simulated diluted bittern, DB (252×10^{-3} mol/L $MgCl_2\cdot6H_2O$, 77×10^{-3} mol/L KCl, 25×10^{-3}

mol/L $MgSO_4 \cdot 7H_2O$, 26×10^{-3} mol/L NaCl, and 8×10^{-3} mol/L NH_4Cl). Further information on the composition of WSRW and DB can be found in the Supplementary Material. Table S5 of the Supplementary Material summarizes the conditions for experiments presented in the following Figures.

4. Results and discussion

4.1. Driver Ion Concentration Gradient Drives Transport of Orthophosphate Across the Anion Exchange Membrane

Donnan dialysis experiments were conducted using an initial FS of 30×10^{-3} mol/L $H_2PO_4^-$ and RS of 600×10^{-3} mol/L Cl^-. Note that the FS simulates the pH and $[H_2PO_4^-]$ of fresh urine, with $H_2PO_4^-$ being the predominant form of orthophosphate species at pH = 6.0. The RS replicates $[Cl^-]$ in seawater. Figure 2 shows $[H_2PO_4^-]$ in the feed and receiver solutions, indicated by subscripts FS and RS, respectively (solid blue square and open blue circle symbols), and $[Cl^-]$ in the FS (open gray square symbols) as a function of time during DD operation. Because of the large driver ion concentration difference across the membrane, i.e., $[Cl^-]_{RS,0} - [Cl^-]_{FS,0}$, Cl^- permeates from the RS to the lower concentration FS. Na^+ cations are rejected by the AEM; thus, to maintain electroneutrality, one $H_2PO_4^-$ ion from the FS exchanges with one Cl^- ion from the RS, as demonstrated by nearly equal $[H_2PO_4^-]_{RS}$ and $[Cl^-]_{FS}$ throughout the DD experiment ($<1.5 \times 10^{-3}$ mol/L difference). Further, $[H_2PO_4^-]_{FS}$ decreases at the same rate as $[H_2PO_4^-]_{RS}$ increases, i.e., mole balance is satisfied, with $[H_2PO_4^-]_{FS}V_{FS} + [H_2PO_4^-]_{RS}V_{RS}$ within 5% of $[H_2PO_4^-]_{FS,0}V_{FS,0}$. As more $H_2PO_4^-$ and Cl^- ions are exchanged, the electrochemical potential gradient across the AEM decreases. The reduced driving force lessens the rate of anion exchange, i.e., slopes of the concentration profiles become less steep. Importantly, even after $[H_2PO_4^-]_{RS}$ exceeds $[H_2PO_4^-]_{FS}$

(at ≈3 h), $H_2PO_4^-$ continues to be transported from the feed to receiver solution, achieving uphill transport of orthophosphates. Approximately 73% of $H_2PO_4^-$ from the FS was recovered in the RS after 6 h of DD operation in batch mode.

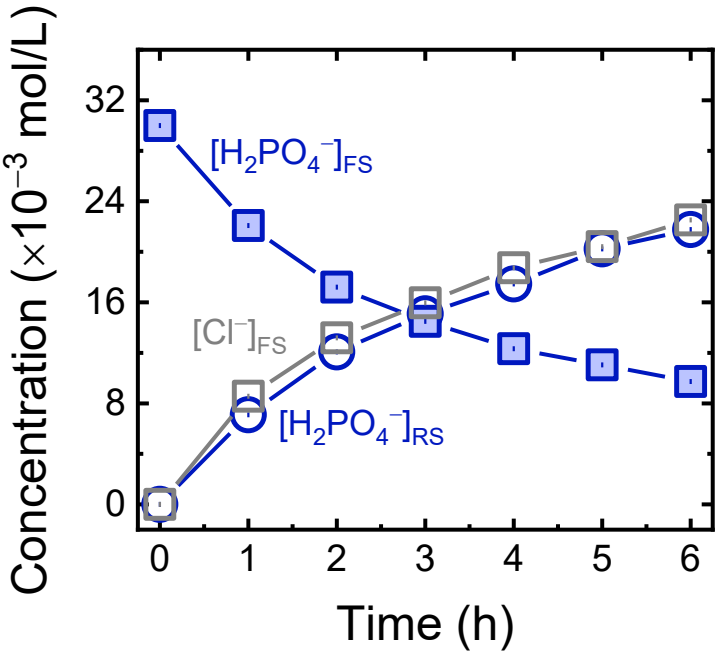

Figure 2. Concentrations of $H_2PO_4^-$ and Cl^- in the FS (solid blue and open gray square symbols, respectively) and $H_2PO_4^-$ concentration in the RS (open blue circles) as a function of time during DD orthophosphate recovery. Feed and receiver solution concentrations are denoted by subscripts FS and RS, respectively. The initial feed and receiver solutions consist of 30×10^{-3} mol/L $H_2PO_4^-$ at pH = 6.0 (16.5×10^{-3} mol/L $Na_2HPO_4\cdot7H_2O$ and 13.5×10^{-3} mol/L H_3PO_4) and 600×10^{-3} mol/L NaCl, respectively. Both feed and receiver solution volumes are 20 mL and effective AMV membrane area is 9.0 cm^2.

4.2. Higher Receiver Solution Chloride Concentrations Increase Orthophosphate Recovery

Donnan dialysis experiments were conducted using FS with 30×10^{-3} mol/L TOP, i.e., the $H_xPO_4^{(3-x)-}$ concentration in fresh urine where $H_2PO_4^-$ is the predominant orthophosphate species,

and various initial $[Cl^-]_{RS}$ to investigate the influence of chloride driver ion concentration on orthophosphate recovery. Receiver solutions of 200, 600, and $1{,}000\times10^{-3}$ mol/L NaCl were utilized to simulate potential widely-available low-cost/waste streams of brackish water, seawater, and seawater desalination brine, respectively. Figure 3A presents experimental $[H_xPO_4^{(3-x)-}]_{RS,f}$ at the end of 72 h and predicted $[H_xPO_4^{(3-x)-}]_{RS,f}$ at Donnan equilibrium calculated using eq 2 (patterned and empty blue columns, respectively). Labels above these columns denote percentage difference of experimental $[H_xPO_4^{(3-x)-}]_{RS,f}$ relative to the prediction at Donnan equilibrium.

Theoretical orthophosphates captured in the receiver solution at Donnan equilibrium increase with greater feed concentrations of driver chloride ions: predicted $[H_xPO_4^{(3-x)-}]_{RS,f}$ are 26.1, 28.6, and 29.1×10^{-3} mol/L for $[Cl^-]_{RS,0}$ of 200, 600, and $1{,}000\times10^{-3}$ mol/L, respectively. The FS is constant across all operations. Therefore, higher $[Cl^-]_{RS,0}$ generates larger driver ion concentration gradients, i.e., $[Cl^-]_{RS}-[Cl^-]_{FS}$, and results in increased driving forces for Cl^- permeation from the high concentration FS to the lower concentration RS. Correspondingly, there is a greater exchange of $H_xPO_4^{(3-x)-}$ ions to the RS (eq 2). The DD experiments exhibited this increasing trend of $[H_xPO_4^{(3-x)-}]_{RS,f}$ with larger $[Cl^-]_{RS,0}$ (patterned blue columns of Figure 3A). However, the observed $[H_xPO_4^{(3-x)-}]_{RS,f}$ were below the predicted values by ≈8–15%, with the improvements being less marked at greater $[Cl^-]_{RS,0}$, e.g., raising $[Cl^-]_{RS,0}$ from 200 to $1{,}000\times10^{-3}$ mol/L increases $[H_xPO_4^{(3-x)-}]_{RS,f}$ by 3.7%, lower than the theoretical enhancement of 11.3%.

$[H_xPO_4^{(3-x)-}]_{RS,f}$ for the three different $[Cl^-]_{RS,0}$ are lower than theoretical final concentrations due to dilution by simultaneous water transport from FS to RS and imperfect cation exclusion by the AEM. The high concentration of NaCl in the RS generates an osmotic pressure gradient that drives water permeation from FS to RS, i.e., osmosis. Additionally, electro-osmosis, where water molecules are dragged along with the permeating charged ions, contributes to water

transport (J. Veermana et al., 2009; Spiegler, 1958; Yip and Elimelech, 2012). Electro-osmosis due to $H_xPO_4^{(3-x)-}$ flux from FS to RS is opposite in direction to water transport by Cl^- flux (and Na^+ flux, explained next) from RS to FS. Net electro-osmosis is <10% of the measured water permeation; therefore, the contribution from the phenomenon is relatively minor and osmosis is the primary driver of water transport. The RS volume increased by 5.3–21% at the end of the DD experiments performed here. Water flux dilutes the RS and consequently lowers the TOP concentration. Note that, in contrast, minimal water transport was measured for the experiment presented in Figure 2 because the experiment duration was comparatively shorter (6.0 h instead of 72 h).

Additionally, co-ions are not completely rejected by ion-exchange membranes (Beck and Ernst, 2015; Pessoa-Lopes et al., 2016). The Na^+ concentration gradient set up by the high [NaCl] in the RS results in Na^+ permeation from RS to FS, i.e., co-ion (cation) leakage. To maintain electroneutrality, every Na^+ ion that leaks across the AEM compels one Cl^- ion to permeate in the same direction; therefore $H_2PO_4^-$ and Cl^- are transported below equimolar ratio and $[Cl^-]_{FS,f}+[H_xPO_4^{(3-x)-}]_{FS,f} > [H_xPO_4^{(3-x)-}]_{FS,0}$. The cation leakage reduces Cl^- ions in RS that are available to exchange with $H_xPO_4^{(3-x)-}$ ions in the FS, thus detrimentally lowering $[H_xPO_4^{(3-x)-}]_{RS,f}$. Na^+ transport was not specifically characterized in the experiments, but was estimated to be in the approximate region of 5% of anion transport, based on the membrane permselectivity of ≈0.95 reported in the manufacturer's specifications. Both water and co-ion leakage are not accounted for in eq 2 and cause the experimental $[H_xPO_4^{(3-x)-}]_{RS,f}$ to deviate below the predicted Donnan equilibrium. Note that transport of Cl^- from RS to FS and $H_2PO_4^-$ from FS to RS were nearly identical during the 6 h of DD operation presented in Figure 2; however, given the relatively longer duration of the phosphate recovery experiments presented in Figure 3A (72 h), cumulative co-ion

transport is more pronounced. Additionally, the ballpark estimate of cation leakage is consistent with the deviations between experimental and predicted orthophosphate concentrations.

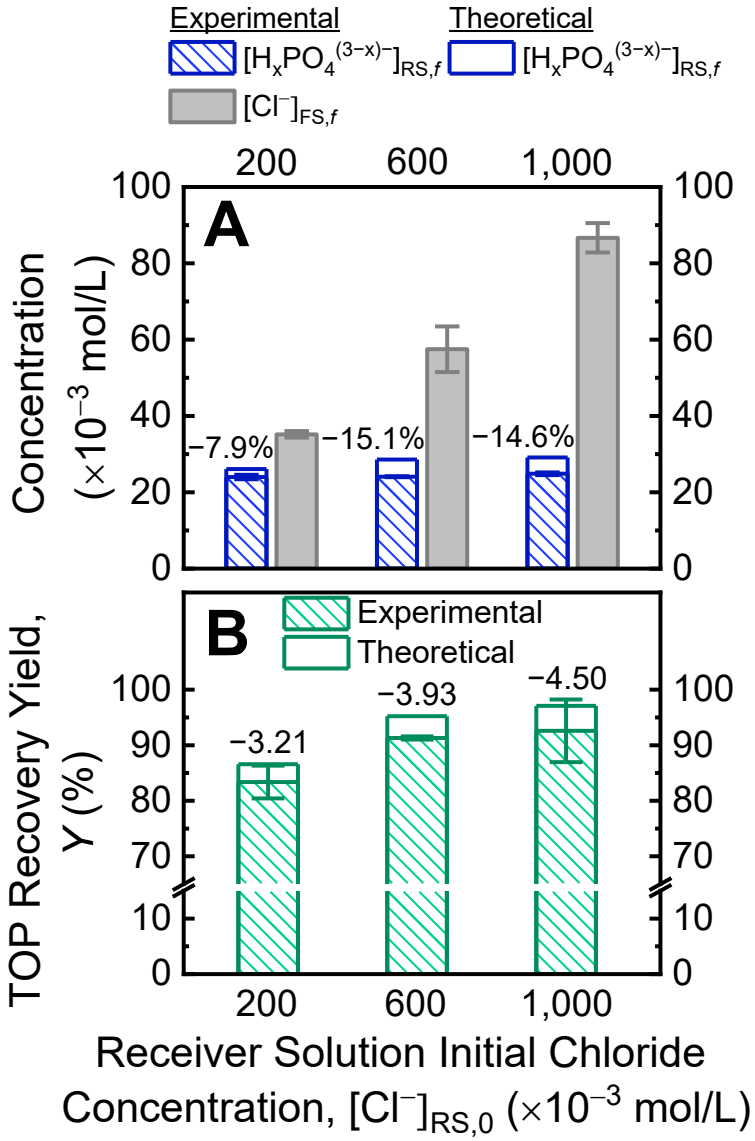

Figure 3. A) $[H_xPO_4^{(3-x)-}]_{RS,f}$ and $[Cl^-]_{FS,f}$ (patterned blue and gray columns, respectively) in DD with different initial NaCl concentrations in the receiver solution. Predicted $[H_xPO_4^{(3-x)-}]_{RS,f}$ at Donnan equilibrium, calculated using eq 2, are depicted by the empty blue columns. Labels above the columns indicate the percentage of predicted $[H_xPO_4^{(3-x)-}]_{RS,f}$ experimentally captured in the RS. B) Experimental and predicted orthophosphate recovery yields, *Y*, (patterned and empty green columns, respectively) in DD with the different $[Cl^-]_{RS,0}$. The experimental *Y* were calculated from measured

$[H_xPO_4^{(3-x)-}]_{RS,f}$ and accounting for osmotic water flux the FS to the RS. Labels above the columns signify the percent decrease in $H_xPO_4^{(3-x)-}$ experimentally captured in the RS relative to theoretical prediction (based on eq 2). Initial feed solution contains 30×10^{-3} mol/L $H_2PO_4^-$ at pH = 6.0 (i.e., same composition as the FS of Figure 2). Receiver solutions with initial concentrations of 200, 600, and $1{,}000\times10^{-3}$ mol/L NaCl to simulate brackish water, seawater, and seawater desalination brine, respectively, were investigated. In all operations V_{FS}/V_{RS} is 1:1. All experiments utilized AMV membranes. Data points and error bars are means and standard deviations, respectively, of duplicate experiments.

$H_xPO_4^{(3-x)-}$ experimentally captured in the RS are 7.91%, 15.1%, and 14.6% lower than predicted for $[Cl^-]_{RS,0}$ of 200, 600, and 1,000 $\times10^{-3}$ mol/L, respectively. Deviations of the experimental $[H_xPO_4^{(3-x)-}]_{RS,f}$ from theoretical values (eq 2) are larger with $[Cl^-]_{RS,0}$ of 600 and $1{,}000\times10^{-3}$ mol/L compared to 200×10^{-3} mol/L (experimental $[H_xPO_4^{(3-x)-}]_{RS,f}$ of $[Cl^-]_{RS,0}$ = 1,000 mol/L being marginally smaller than $[Cl^-]_{RS,0}$ = 600 mol/L is likely attributed to inevitable experimental uncertainties inherent to the measurement techniques). The greater deficits are due to both water permeation from FS to RS (quantified by measuring changes in the solution volumes) and cation leakage from RS to FS being more prominent in operations with higher $[Cl^-]_{RS,0}$. Osmotic pressure is essentially proportional to [NaCl] and are 9.91, 29.7, and 49.6 bar for 200, 600, and $1{,}000\times10^{-3}$ mol/L NaCl, respectively. As a result of the greater osmotic pressure difference between the RS and FS, increased water permeation is observed when $[Cl^-]_{RS,0}$ is higher; net water fluxes are 1.93×10^{-2}, 6.37×10^{-2}, and 7.10×10^{-2} L/m^{2}h for initial RS of 200, 600, and $1{,}000\times10^{-3}$ mol/L NaCl, respectively. Additionally, Na^+ leakage is more exacerbated with conditions of higher initial RS [NaCl] due to increased Na^+ concentration gradients.(Beck and Ernst, 2015; Pessoa-Lopes et al., 2016) Consequently, the undesired co-permeation of Cl^- is elevated. In principle, $[Cl^-]_{FS,f}$ (gray columns in Figure 3A) should be equivalent to

380 $[H_xPO_4^{(3-x)-}]_{RS,f}$ because the predominant form of orthophosphate in the FS is monovalent $H_2PO_4^-$,
381 and therefore electroneutrality dictates a 1:1 exchange of Cl^- and $H_2PO_4^-$. However,
382 experimentally, $[Cl^-]_{FS,f} > [H_xPO_4^{(3-x)-}]_{RS,f}$ due to the Na^+ and Cl^- leakage from RS to FS and water
383 flux from FS to RS. Furthermore, the divergences between $[Cl^-]_{FS,f}$ and $[H_xPO_4^{(3-x)-}]_{RS,f}$ are larger
384 at higher $[Cl^-]_{RS,0}$ as co-ion leakage and osmosis, are more exacerbated. Although increasing
385 $[Cl^-]_{RS,0}$ resulted in higher TOP concentrations recovered in the receiver solution, the greater
386 deviations between experimental and predicted DD performance also indicate that the
387 inefficiencies of water and co-ion leakage are more pronounced.

388 Recovery yield, *Y*, is defined as the percentage of orthophosphate moles from the initial FS
389 that are recovered in the RS and is presented in Figure 3B, with patterned and empty green columns
390 denoting experimental and predicted *Y*, respectively. Experimental *Y* is calculated using the
391 product of TOP concentration and solution volume at the end of the test ($[H_xPO_4^{(3-x)-}]_{RS,f}V_{RS,f}$),
392 i.e., the effects of osmotic and electro-osmotic water transport are accounted for. Labels above the
393 columns are the differences between experimental and predicted *Y*. The experimental
394 orthophosphate recovery yields are very close to *Y*s predicted at Donnan equilibrium using eq 2
395 (within 5%). The minor shortfalls in recovery yield are attributed to Na^+ leakage and Cl^- co-
396 permeation. Despite the imperfect permselectivity of the AEM, experimental *Y*s are high and
397 exceed 90% for $[Cl^-]_{RS,0}$ of 600×10^{-3} and $1{,}000\times10^{-3}$ mol/L. Even the lowest $[Cl^-]_{RS,0}$ of 200×10^{-3}
398 mol/L produced *Y* of 83%. The high yields achieved signify that DD can be a promising technique
399 for orthophosphate recovery. Increasing $[Cl^-]_{RS,0}$ improves *Y*, but with diminishing returns. For
400 example, raising $[Cl^-]_{RS,0}$ from 200×10^{-3} to 600×10^{-3} mol/L increases experimental *Y* by 9.5%.
401 However, further increasing $[Cl^-]_{RS,0}$ to $1{,}000\times10^{-3}$ mol/L only marginally improved the
402 orthophosphate recovery yield by 1.4% (this trend is also predicted by the Donnan equilibrium

theory of eq 2). Subsequent phosphate recovery experiments will, thus, utilize $[Cl^-]_{RS,0} = 600\times10^{-3}$ mol/L.

4.3. Donnan Dialysis can Enrich Orthophosphate in the Receiver Solution

It is advantageous to produce concentrated orthophosphate solutions to be utilized in downstream applications as fertilizer. Orthophosphate can be enriched in the RS (i.e., $[H_xPO_4^{(3-x)-}]_{RS,f} > [H_xPO_4^{(3-x)-}]_{FS,0}$) by using a smaller RS volume relative to FS, based on the Donnan equilibrium (eqs S14–17 of the Supplementary Material). DD experiments were conducted using different V_{FS}/V_{RS} of 1, 2, and 4. The FS contains 30×10^{-3} mol/L of $H_xPO_4^{(3-x)-}$ and the RS has 600×10^{-3} mol/L of Cl^-. Figure 4 presents experimental $[H_xPO_4^{(3-x)-}]_{RS,f}$ as patterned blue columns, and predicted $[H_xPO_4^{(3-x)-}]_{RS,f}$ are indicated by the blue dashed line (left vertical axis). Labels in the columns denote enrichment factors, defined as $[H_xPO_4^{(3-x)-}]_{RS,f}/[H_xPO_4^{(3-x)-}]_{FS,0}$. Experimental and predicted recovery yields of $H_xPO_4^{(3-x)-}$, Y, are green square symbols and green dashed line, respectively (right vertical axis).

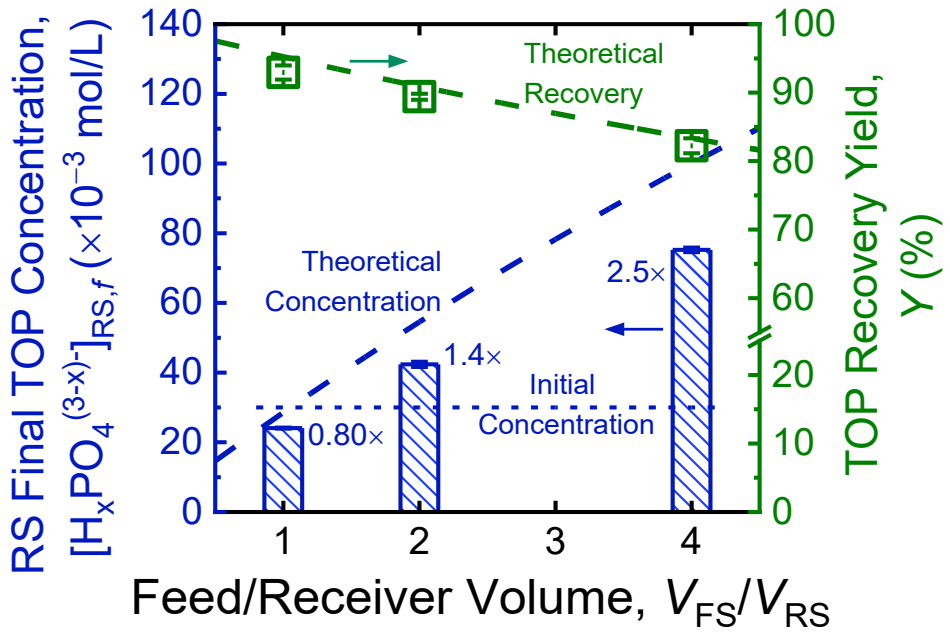

Figure 4. Receiver solution final TOP concentration, $[H_xPO_4^{(3-x)-}]_{RS,f}$ (blue columns, left vertical axis), and orthophosphate recovery yields, Y (green square symbols, right vertical axis), as a function of V_{FS}/V_{RS}. Experimental Y is calculated using $[H_xPO_4^{(3-x)-}]_{RS,f}V_{RS,f}$ and, therefore, accounts for water transport from the FS to the RS due to osomosis and electro-osmosis. Predicted $[H_xPO_4^{(3-x)-}]_{RS,f}$ and recovery yields at Donnan equillibrium, calculated using eqs S14–17 in the Supplementary Material, are depicted as blue and green dashed lines, respectively. The initial feed and receiver solutions are the same as the FS and RS of Figure 2. For comparison, the initial total orthophosphate concentration in the simulated urine feeds is depicted as a dotted blue line. Enrichment factors, defined as $[H_xPO_4^{(3-x)-}]_{RS,f}/[H_xPO_4^{(3-x)-}]_{FS,0}$, are indicated in the blue columns. Experimental Y is $[H_xPO_4^{(3-x)-}]_{RS,f}V_{RS,f}$ and, therefore, accounts for osmotic water flux from the FS to the RS. All experiments utilized AMV membranes. Data points and error bars are means and standard deviations, respectively, of duplicate experiments.

Because DD can enable uphill transport of ions from FS to RS, the recovered orthophosphate can be concentrated in a small volume of RS. Enrichment factors of 1.4 and 2.5 were achieved in experiments with V_{FS}/V_{RS} of 2 and 4, respectively. However, experimental $[H_xPO_4^{(3-x)-}]_{RS,f}$ and enrichment factors are lower than predictions by Donnan equilibrium. Eq S8 predicts enrichment factors of 1.8 and 3.3 at Donnan equilibrium with V_{FS}/V_{RS} = 2 and 4, respectively. These deviations are primarily due to water permeation diluting the orthophosphates captured in the RS. Furthermore, the dilution effect is more pronounced at higher V_{FS}/V_{RS}, where osmotic water flux from FS to RS mixes with relatively smaller volumes of RS. As a result, the deviations of experimental $[H_xPO_4^{(3-x)-}]_{RS,f}$ from predicted values are detrimentally elevated with increased V_{FS}/V_{RS} and are −15.7%, −22.3%, and −24.8% for V_{FS}/V_{RS} of 1, 2, and 4, respectively. However, similar to the results presented in Figure 3, experimental recovery yields (green square symbols in Figure 4) are comparable to theoretical Y at Donnan equilibrium (<3% difference between green square symbols and green dashed lines), as water permeation is accounted for in

the determination of moles of TOP recovered. This minor difference is attributed to Na^+ leakage and Cl^- co-permeation, i.e., imperfect AEM permselectivity,(Beck and Ernst, 2015; Pessoa-Lopes et al., 2016) which results in reduced driving force available for $H_xPO_4^{(3-x)-}$ transport.

Varying V_{FS}/V_{RS} produces a tradeoff between enrichment and recovery yield, as predicted by the Donnan equilibrium theory (eq S14–17): increasing V_{FS}/V_{RS} enhances the enrichment factor, but the recovery yield is slightly compromised (dashed blue line and dashed green line in Figure 4 exhibit positive and negative slopes, respectively). This is because with a relatively smaller receiver solution volume, the initial ratio of moles of Cl^- in the RS to moles of $H_xPO_4^{(3-x)-}$ in the FS (i.e., $[Cl^-]V_{RS}$:$[H_xPO_4^{(3-x)-}]_{FS,0}V_{FS}$) is lower. Therefore, there are fewer available driver Cl^- ions to exchange with target $H_2PO_4^-$ ions, and the achievable Y is decreased. Nevertheless, it can be overall advantageous to use a higher V_{FS}/V_{RS}, if the benefit from a greater enrichment factor outweighs the loss in recovery yield. For example, compared to V_{FS}/V_{RS} = 1, experimental enrichment factor increased by 76.0% and 212.4% at V_{FS}/V_{RS} of 2 and 4, respectively, while experimental Y only decreased by 5.9% and 11.7%. Furthermore, the highest enrichment factor (at V_{FS}/V_{RS} = 4) was still achieved with adequately high orthophosphate recovery >80%.

4.4. Competing Anions in the Urine Feed Solutions Lower Orthophosphate Transport and Recovery

Results presented thus far utilized a feed solution with TOP concentration of fresh urine, i.e., orthophosphate as the sole anion. However, actual fresh urine contains orthophosphate, sulfate, and chloride anions, and hydrolyzed urine additionally has significant bicarbonate concentration (Fittschen and Hahn, 1998; Larsen et al., 2013; Simha and Ganesapillai, 2017; Udert et al., 2003a). To examine the effects of other anions on orthophosphate recovery, DD experiments were

conducted using simulated fresh urine and hydrolyzed urine (anion compositions are summarized in Table 1), for comparison with the TOP-only solution. In all operations, the RS has 600×10^{-3} mol/L of Cl^-. Figure 5A shows experimental $[H_xPO_4^{(3-x)-}]_{RS,f}$, $[SO_4^{2-}]_{RS,f}$, and $[HCO_3^-]_{RS,f}$ as patterned blue, orange, and red columns, respectively. Empty columns of the respective colors signify concentrations in the RS at Donnan equilibrium (determined using eqs S9–13 of the Supplementary Material). Labels above the arrows designate the percent change in experimental $[H_xPO_4^{(3-x)-}]_{RS,f}$ achieved in DD relative to orthophosphate-only feed solution.

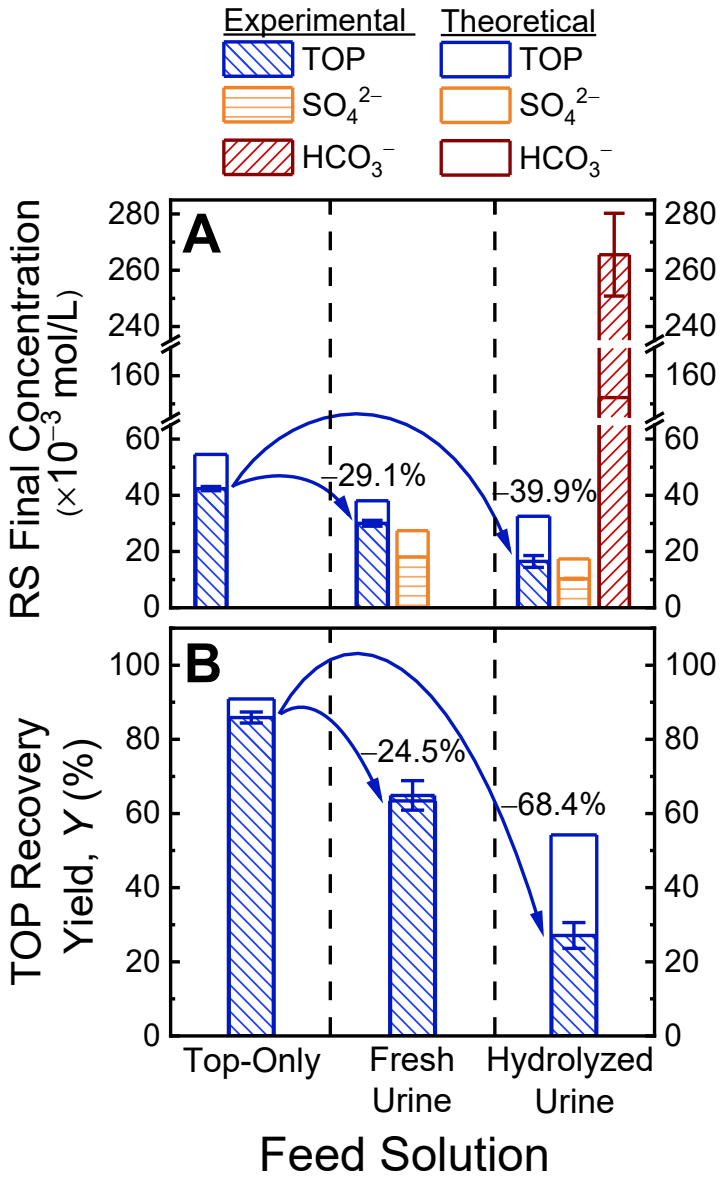

Figure 5. A) Final RS concentrations, $[H_xPO_4^{(3-x)-}]_{RS,f}$, $[SO_4^{2-}]_{RS,f}$, and $[HCO_3^-]_{RS,f}$, and B) orthophosphate recovery yields in TOP recovery experiments with different urine matrices as initial feed solutions. The three FS are: orthophosphate anion-only, fresh urine, and hydrolyzed urine. $[H_xPO_4^{(3-x)-}]_{FS,0}$ of all three FS are 30×10^{-3} mol/L. Simulated fresh urine contains 16×10^{-3} mol/L SO_4^{2-} and 100×10^{-3} mol/L Cl^- anions as well as $H_xPO_4^{(3-x)-}$, whereas simulated hydrolyzed urine additionally has 250×10^{-3} mol/L HCO_3^-. Note that the transport of water from feed solution to receiver solution is accounted for in the experimental orthophosphate recovery yields. Predicted final RS concentrations

and predicted orthophosphate recovery yields at Donnan equilibrium, calculated using eqs S14–17 in the Supplementary Material, are depicted as empty columns. The labels above the columns indicate the change relative to the orthophosphate-only FS. All experiments were operated with V_{FS}/V_{RS} equal to 2 and 600×10^{-3} mol/L NaCl as the receiver solution. All experiments utilized AMV membranes. Data points and error bars are means and standard deviations, respectively, of duplicate experiments.

Theoretical $[H_xPO_4^{(3-x)-}]_{RS,f}$ are 30.3% and 40.3% lower in operations with fresh and hydrolyzed urine, respectively, relative to TOP-only FS (empty blue columns in Figure 5A). In DD with fresh urine, both SO_4^{2-} and $H_xPO_4^{(3-x)-}$ ions can transport from the FS to the RS to balance Cl^- transport from RS to FS and maintain net electroneutrality. Therefore, SO_4^{2-} ions compete with target $H_xPO_4^{(3-x)-}$ ions to exchange with Cl^- ions. Moreover, SO_4^{2-} is a divalent anion. Thus, two Cl^- ions are required to exchange with one SO_4^{2-} ion to achieve charge balance, which further limits Cl^- ions available to exchange with $H_xPO_4^{(3-x)-}$. Additionally, the inclusion of Cl^- ions in the fresh urine matrix also decreases the chloride concentration gradient, $[Cl^-]_{RS}-[Cl^-]_{FS}$, which lowers the total Cl^- ions that will be transported from RS to FS at Donnan equilibrium. The decreased driver ion transport further decreases the transport of target ion $H_xPO_4^{(3-x)-}$ from the FS to RS. Thus, both the competition with SO_4^{2-} ions and the weakened driving force give rise to the decline of predicted $[H_xPO_4^{(3-x)-}]_{RS,f}$ in operations with fresh urine relative to TOP-only.

In DD with hydrolyzed urine, HCO_3^- ions pose additional competition for exchange with the driver Cl^- ions, which leads to further reduction of predicted $[H_xPO_4^{(3-x)-}]_{RS,f}$ relative to FS of TOP-only. For the same reason, predicted $[SO_4^{2-}]_{RS,f}$ in operations with hydrolyzed urine is 36.7% lower than with fresh urine (HCO_3^- ion competition also impacts SO_4^{2-} transport). The concentration of HCO_3^- in hydrolyzed urine, 250×10^{-3} mol/L, is nearly 1 order of magnitude higher than $H_xPO_4^{(3-x)-}$ and over 1 order of magnitude higher than SO_4^{2-} (30×10^{-3} mol/L and 16×10^{-3} mol/L, respectively). As a result, the exchange of HCO_3^- with Cl^- is expected to dominate

503 over the exchange with other anions in the FS, yielding predicted $[HCO_3^-]_{RS,f} >> [H_xPO_4^{(3-x)-}]_{RS,f} >$
504 $[SO_4^{2-}]_{RS,f}$. To uncouple the relative impact of these three factors (i.e., i) competition with SO_4^{2-}
505 ions, ii) competition with HCO_3^- ions, and iii) the weakened driving force due to Cl^- ions in the
506 FS) on orthophosphate recovery, further analysis was performed (detailed in the Supplementary
507 Material), and the competition posed by HCO_3^- in hydrolyzed urine was found to be the main
508 reason projected $[H_xPO_4^{(3-x)-}]_{RS,f}$ is significantly lower than in DD with TOP-only FS (Figure S1
509 of the Supplementary Material).

510 Consistent with the Donnan equilibrium predictions, experimental $[H_xPO_4^{(3-x)-}]_{RS,f}$ in DD
511 with fresh and hydrolyzed urine are 29.1% and 39.9% lower, respectively, relative to TOP-only
512 feed solution (Figure 5A). However, all experimental $[H_xPO_4^{(3-x)-}]_{RS,f}$ are lower than theoretical
513 values at Donnan equilibrium (−22.3%, −21.0%, and −49.4% with TOP-only FS, fresh urine, and
514 hydrolyzed urine, respectively). Similarly, $[SO_4^{2-}]_{RS,f}$ in operations with fresh and hydrolyzed
515 urine are 34.1% and 40.5% lower, respectively, than predicted. As discussed earlier, these
516 differences are caused by water permeation from FS to RS diluting the ions captured in the RS and
517 co-ion leakage of Na^+ from RS to FS lowering anion transport from FS to RS.

518 However, experimental $[HCO_3^-]_{RS,f}$ with hydrolyzed urine is significantly higher than
519 predicted (+60.9%, red columns in Figure 5A). At the same time, experimental $[H_xPO_4^{(3-x)-}]_{RS,f}$ in
520 DD with hydrolyzed urine resulted in considerably larger deviations from Donnan equilibrium
521 values (−49.4%) than with TOP-only feed solution and fresh urine (−22.3% and −21.0%,
522 respectively). One possible explanation for these observations is that the hydrolyzed urine
523 experiments were terminated prior to actual equilibrium. The experimental protocol used
524 $[H_xPO_4^{(3-x)-}]_{RS}$ to assess the progress of ions transport in DD, with test runs ending when
525 orthophosphate concentrations stagnated (< 5% change over three consecutive measurements). If

the transport of HCO_3^- ions from the FS to RS is much faster than the transport of $H_xPO_4^{(3-x)-}$ ions in the same direction, $[H_xPO_4^{(3-x)-}]_{RS}$ can appear to level-off and trigger premature termination of the experiments. Ion transport kinetics will be further evaluated in the following subsection. To explore this postulation, $\left(\left[H_xPO_4^{(3-x)-}\right]_{FS}/\left[H_xPO_4^{(3-x)-}\right]_{RS}\right)^{1/(3-x)}$ and $\left[HCO_3^-\right]_{FS}/\left[HCO_3^-\right]_{RS}$ were calculated using concentrations at the end of the experimental runs (note that the predominant form of $H_xPO_4^{(3-x)-}$ in hydrolyzed urine of pH = 9.2 is HPO_4^{2-} and, therefore, x = 1). At Donnan equilibrium, the fractions should be equal. However, the values for HPO_4^{2-} and HCO_3^- are 1.15 and 0.445, respectively, indicating that the system has not fully equilibrated at the end point of the experiment. Furthermore, $\left[HCO_3^-\right]_{FS}/\left[HCO_3^-\right]_{RS} < \left(\left[HPO_4^{2-}\right]_{FS}/\left[HPO_4^{2-}\right]_{RS}\right)^{1/2}$ suggests that experimental $[HCO_3^-]_{RS}$ at end of the test run is higher than theoretical concentration at Donnan equilibrium. Allowing the DD experiments to proceed further can possibly result in redistribution of the ions between the FS and RS, such that $\left[HCO_3^-\right]_{FS}/\left[HCO_3^-\right]_{RS}$ and $\left(\left[HPO_4^{2-}\right]_{FS}/\left[HPO_4^{2-}\right]_{RS}\right)^{1/2}$ are similar.

Figure 5B presents experimental and predicted orthophosphate recovery yields, *Y* (patterned and empty blue columns, respectively); note that *Y* accounts for water transport (as discussed earlier). Labels above the arrows designate the percent reduction in experimental *Y* relative to orthophosphate-only FS. Recovery yield trends are generally similar to $[H_xPO_4^{(3-x)-}]_{RS,f}$ trends. Specifically, *Y* are 24.5% and 68.4% lower with fresh and hydrolyzed urine, respectively, relative to DD with TOP-only FS, which qualitatively agrees with theoretical predictions of 30.3% and 40.3% reduction. Experimental DD with TOP-only feed solutions and fresh urine deviate slightly from predicted *Y* at Donnan equilibrium (<3%). As previously discussed, Na^+ leakage

547 from RS to FS results in less $H_xPO_4^{(3-x)-}$ ion transport from FS to RS, which explains the
548 experimental *Y* being slightly lower than the predicted value for DD with TOP-only FS. For fresh
549 urine, co-ion leakage is lower because the Na^+ present in the FS reduces the Na^+ concentration
550 gradient, which drives co-ion permeation. Therefore, the experimental and predicted *Y*s are
551 comparable for DD with fresh urine (minor difference is due to unavoidable random fluctuations
552 in experimental measurements). In contrast, *Y* is significantly lower than the theoretical recovery
553 yield at Donnan equilibrium for hydrolyzed urine (50.0% lower). As conjectured in the preceding
554 paragraph, the substantially greater discrepancy is possibly explained by the premature termination
555 of the DD experiment before the ion concentrations were fully equilibrated.

556 *4.5. Orthophosphate Fluxes are Diminished by the Competing Anions*

557 Parallel DD kinetics experiments were conducted with the same initial feed solutions
558 presented in Figure 5, i.e., TOP-only FS, fresh urine, and hydrolyzed urine. To elucidate the
559 impacts of individual ionic species in the urine matrix on ion fluxes, additional DD kinetic
560 experiments were carried out with feed solutions of $H_xPO_4^{(3-x)-} + SO_4^{2-}$ and $H_xPO_4^{(3-x)-} + Cl^-$. In
561 all operations, the RS has 600×10^{-3} mol/L of Cl^- and $V_{FS}/V_{RS} = 1$. Figure 6 shows molar ion fluxes,
562 J_i, of $H_xPO_4^{(3-x)-}$, SO_4^{2-}, and HCO_3^- from FS to RS (subscript *i* is P, S, and C, respectively) as
563 patterned blue, orange, and red columns, respectively; labels above blue columns indicate
564 reduction in J_P relative to DD with the orthophosphate-only FS.

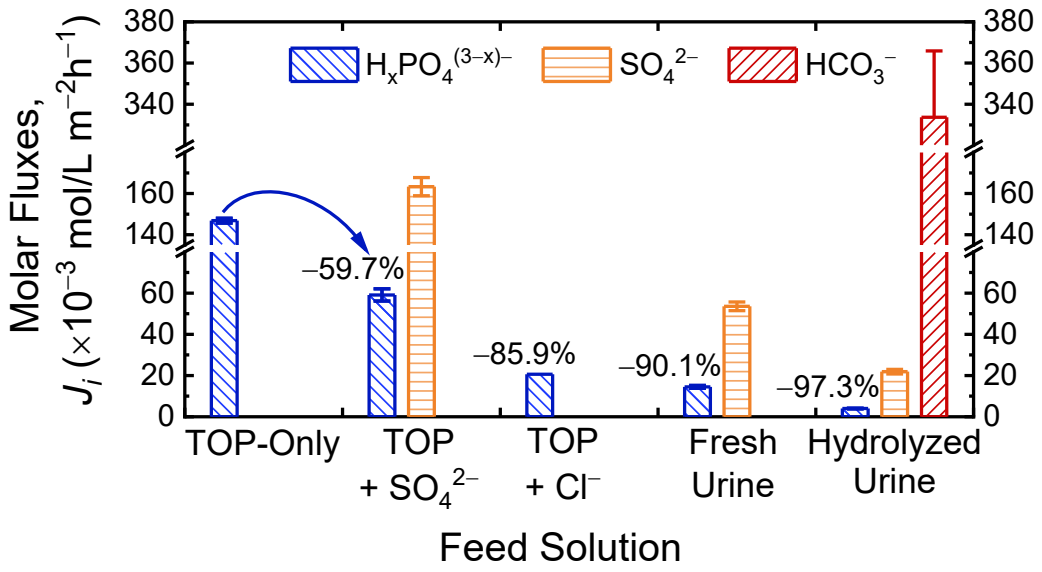

Figure 6. $H_xPO_4^{(3-x)-}$, SO_4^{2-}, and HCO_3^- anion fluxes from FS to RS, J_i, in kinetic experiments with different urine matrices as initial feed solutions. The anions of the five FS are: i) orthophosphate only, ii) orthophosphate and sulfate, iii) orthophosphate and chloride, iv) orthophosphate, sulfate, and chloride (fresh urine), and v) orthophosphate, sulfate, bicarbonate, and chloride (hydrolyzed urine). Labels above the columns indicate the change in flux relative to the orthophosphate-only feed solutions. $[H_xPO_4^{(3-x)-}]_{FS,0}$ of all FS are 30×10^{-3} mol/L. When present in the FS, SO_4^{2-}, Cl^-, and HCO_3^- concentrations are 16×10^{-3}, 100×10^{-3}, and 250×10^{-3} mol/L, respectively. V_{FS}/V_{RS} = 1 and receiver solutions are 600×10^{-3} mol/L NaCl for all experiments. All experiments utilized AMV membranes. Data points and error bars are means and standard deviations, respectively, of duplicate experiments.

As observed with experimental $[H_xPO_4^{(3-x)-}]_{RS,f}$ and Y (Figures 5A and B), J_P is reduced in DD with simulated fresh or hydrolyzed urine relative to orthophosphate-only FS (90.1% and 97.3% lower, respectively). However, the decreases in anion fluxes with the inclusion of SO_4^{2-}, Cl^-, and HCO_3^- are more drastic than the observed decreases in $[H_xPO_4^{(3-x)-}]_{RS,f}$ and Y. Introducing SO_4^{2-} to the FS containing only orthophosphate ions diminishes J_P by 59.7%, whereas the isolated inclusion of Cl^- decreases J_P by 85.9%. These reductions in J_P qualitatively mirror the reductions

582 in $[H_xPO_4^{(3-x)-}]_{RS,f}$ at Donnan equilibrium, i.e., presence of Cl^- and SO_4^{2-} in the FS both lower
583 fluxes and final concentrations, but the influence of Cl^- ions is greater in magnitude. The effects
584 of the competing ions on J_P are similar to the impacts on $[H_xPO_4^{(3-x)-}]_{RS,f}$: the presence of SO_4^{2-}
585 poses competition for $H_xPO_4^{(3-x)-}$ permeation from FS to RS, whereas Cl^- in the FS reduces the
586 electrochemical potential gradient driving Cl^- transport from RS to FS and consequently lowers
587 $H_xPO_4^{(3-x)-}$ permeation. Further analysis indicates that the lessened $\Delta[H_xPO_4^{(3-x)-}]$ does not fully
588 explain the diminished J_P (see Supplementary Material for detailed discussion and results, Table
589 S6 and Figure S2).

590 Instead, the observed differences in J_P could possibly be explained by different affinities
591 of the various ions to sorb into the anion exchange membrane. Specifically, if other anions in the
592 FS, such as SO_4^{2-} and Cl^-, more preferentially partition into the membrane than $H_xPO_4^{(3-x)-}$, the
593 relative concentration of orthophosphate ions within the IEM will be disproportionately lower
594 compared to the feed solution (Malewitz et al., 2007). As flux is directly proportional to the ion
595 concentration in the IEM, J_P will consequently be depressed. Additionally, the higher charge of
596 multivalent ions favors sorption into the charged membrane more than monovalent ions (Galizia
597 et al., 2017). Hence, partitioning of $H_2PO_4^-$, the predominant orthophosphate species, into the IEM
598 matrix can be further hindered by the presence of divalent SO_4^{2-}. To assess this postulation,
599 sorption experiments were conducted for each of the feed solutions (method detailed in the
600 Supplementary Material). Figure S3 in the Supplementary Material presents sorption coefficients,
601 X_i, for $H_xPO_4^{(3-x)-}$, SO_4^{2-}, and Cl (subscript i is P, S, and Cl, respectively) with feed solutions
602 containing different anions. Sorption coefficient is defined as ions sorbed into a unit volume of the
603 membrane normalized by molar concentration in the feed solution. If the AEM does not
604 differentiate between the different ions and ion sorption is solely determined by ion concentrations

in the feed solution, X_i should be similar for the three ions ($H_xPO_4^{(3-x)-}$, SO_4^{2-}, and Cl^-) and across different feed solution compositions. However, experiments utilizing fresh urine FS result in different sorption coefficients with $X_{Cl} > X_S > X_P$. These results demonstrate relative affinities of each ion to the AEM, e.g., sorption coefficient for SO_4^{2-} is 4.26× higher than $H_xPO_4^{(3-x)-}$ in the fresh urine FS. Furthermore, the analysis reveals different sorption coefficients for the same ion across various feed solutions. For example, X_P is 85.0% and 92.8% lower in FS with SO_4^{2-} and Cl^-, respectively, relative to FS containing only orthophosphate. This supports the postulation that SO_4^{2-} and Cl^- ions in the FS significantly outcompete $H_xPO_4^{(3-x)-}$ in sorption into the AEM. Aligned with the observed J_P trend, the addition of Cl^- ions suppresses orthophosphate sorption more than the addition of SO_4^{2-} ions. The high concentration of HCO_3^- ions in hydrolyzed urine lowers J_S by 59.2% relative to fresh urine (further analysis on the detrimental impact of bicarbonate ions can be found in the Supplementary Material). Therefore, it is more advantageous for DD to target fresh urine for orthophosphate recovery.

4.6. Monovalent Ion Permselective Membranes can Improve Selectivity for $H_2PO_4^-$ over other Anions in Urine

Despite fresh urine having a higher concentration of $H_2PO_4^-$ than SO_4^{2-}, sulfate flux in Donnan dialysis is still greater than orthophosphate flux (Figure 6). The conventional anion exchange membrane, Selemion AMV, preferentially permeates SO_4^{2-} over $H_2PO_4^-$ primarily because the membrane has greater affinity to sorb divalent SO_4^{2-} than monovalent $H_2PO_4^-$ (Figure S3). To selectively transport and capture $H_xPO_4^{(3-x)-}$ over SO_4^{2-}, we investigate the use of monovalent ion permselective membranes (MIPMs), specifically Selemion ASVN, for DD recovery of orthophosphates from fresh urine. MIPMs are selective for transport of monovalent

627 ions, such as $H_2PO_4^-$, over multivalent ions, such as SO_4^{2-} (details on the mechanisms of valence-
628 selectivity can be found in literature) (Fan et al., 2022; Lu et al., 2011; Saracco, 1997; Saracco and
629 Zanetti, 1994). Because the predominant orthophosphate species in fresh urine is $H_2PO_4^-$, DD with
630 the ASVN MIPM is expected to improve selectivity for $H_xPO_4^{(3-x)-}$ over SO_4^{2-} relative to the
631 conventional AMV. DD kinetic experiments were conducted with the AMV and ASVN
632 membranes using simulated fresh urines as FS, 600×10^{-3} mol/L Cl^- for RS, and $V_{FS}/V_{RS} = 1$. Figure
633 7A presents the ion fluxes from FS to RS, J_i, and Figure 7B shows ion flux selectivity, defined as
634 the molar ion flux normalized by the sum of two fluxes, J_i/J_T. $H_2PO_4^-$ and SO_4^{2-} fluxes are denoted
635 by blue and orange columns, respectively, whereas patterned and solid columns signify AMV and
636 ASVN, respectively.

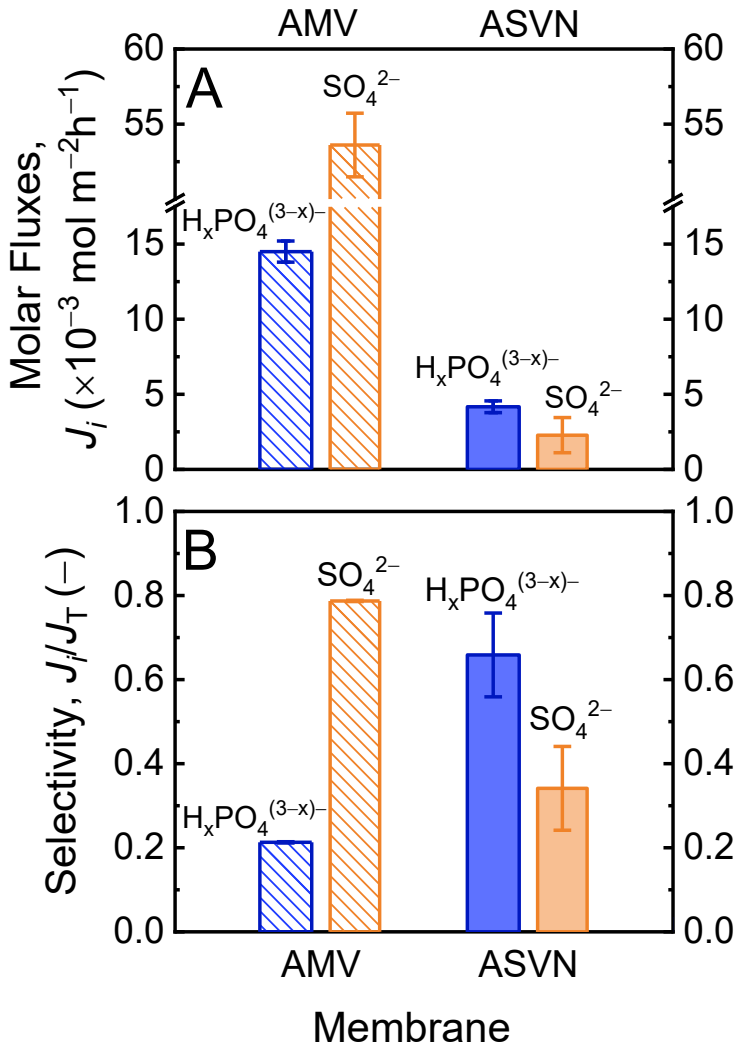

637

638 **Figure 7.** A) Orthophosphate and sulfate molar fluxes from feed solution to receiver solution, J_i, and B)
639 flux selectivity in DD kinetic experiments for conventional anion exchange membrane, AMV, and
640 monovalent ion selective membrane, ASVN. Flux selectivity, J_i/J_T, is defined as flux of the component,
641 J_i, normalized by sum of the two anion fluxes. Blue and orange columns denote $H_2PO_4^-$ and SO_4^{2-},
642 respectively, whereas patterned and solid columns signify AMV and ASVN, respectively. All
643 experiments were operated with V_{FS}/V_{RS} of 1. The feed solution is simulated fresh urine, i.e., 30×10^{-3}
644 mol/L $H_xPO_4^{(3-x)-}$, 16×10^{-3} mol/L SO_4^{2-}, and 100×10^{-3} mol/L Cl^- anions, and 600×10^{-3} mol/L NaCl
645 was used as the receiver solution. Data points and error bars are means and standard deviations,
646 respectively, of duplicate experiments.

Similar to the results presented in Figure 6, Figure 7A shows $J_P < J_S$ in DD with the AMV membrane. Flux selectivity J_P/J_T is 0.21 (Figure 7B), which signifies approximately four SO_4^{2-} ions permeate across the AEM for every $H_2PO_4^-$ ion recovered. In contrast, DD with the monovalent ion-selective ASVN membrane resulted in a reversal in the flux trend, i.e., $J_P > J_S$, with flux selectivity for $H_2PO_4^-$, J_P/J_T, = 0.66. That is, for every two $H_2PO_4^-$ ions recovered, roughly only one SO_4^{2-} anion permeated across. Overall, the ASVN membrane achieved 3.1× higher selectivity for $H_2PO_4^-$ than the AMV membrane. Therefore, ASVN preferentially selected for $H_2PO_4^-$ transport over SO_4^{2-}, resulting in $H_2PO_4^-$ being the predominant anion exchanging from FS to RS with Cl^- in DD orthophosphate recovery.

However, it can be observed from Figure 7A that DD with the ASVN membrane resulted in lower $H_2PO_4^-$ fluxes compared to operation with the AMV membrane. More generally, both ion fluxes are significantly diminished with the MIPM relative to the conventional AEM (71.3 and 95.8% lower for J_P and J_S, respectively). The monovalent ion selective coating on the ASVN membrane is composed of highly crosslinked resin, which creates additional steric hindrance for permeating ions (Fan et al., 2022; Lu et al., 2011; Saracco, 1997; Saracco and Zanetti, 1994). Consequently, the overall ASVN membrane has greater resistance for ion transport compared to the AMV membrane (this is reflected in the manufacturer's specifications on resistance with various salt solutions, summarized in Table S7). Thus, there exists a tradeoff between ion selectivity and permeability: using MIPMs instead of conventional AEMs yields improved monovalent ion selectivity but reduced ion fluxes. In applications of DD for orthophosphate recovery, MIPMs can improve TOP yield, but at the expense of slower kinetics; a lower J_P would necessitate larger membrane areas for the same productivity of orthophosphate recovery.

4.7. Orthophosphate can be Captured as a Fertilizer Solution using Donnan Dialysis

The previously presented results utilized receiver solutions with high Cl^- concentrations to demonstrate the potential of Donnan dialysis to separate orthophosphate from urine, which can have contaminants, e.g., pharmaceuticals, endocrine disrupting compounds, and opportunistic pathogens, that prohibit the direct application of urine for fertilization. Orthophosphate was captured in receiver streams of NaCl solutions for the experiments. However, Na^+ is not well tolerated by most plant species at concentrations > $4.3–13\times10^{-3}$ mol/L, (Genc et al., 2007; Kronzucker et al., 2013) i.e., the eventual DD receiver solutions contain too much sodium. One option to exclude Na^+ is to precipitate phosphate fertilizers as mineral solids, such as struvite, $NH_4MgPO_4\cdot6H_2O$, and potassium magnesium phosphate, $KMgPO_4\cdot6H_2O$, from the TOP-enriched RS by adding Mg^{2+} and NH_4^+ or K^+. As highlighted in the Introduction section, some studies reported the presence of contaminants in phosphate minerals directly precipitated from urine (Boer et al., 2018; Kemacheevakul et al., 2015; Lahr et al., 2016; Mullen et al., 2017; Ronteltap et al., 2007a; Tang et al., 2019). The anion exchange membrane in DD serves as a barrier, retaining the contaminants of concern in the urine feed (Arola et al., 2019; Banasiaka et al., 2011; Ma et al., 2021a; Ma et al., 2021b; Pronk et al., 2006; Vanoppen et al., 2015). Therefore, utilizing Donnan dialysis to separate orthophosphate from the urine matrix prior to mineral precipitation can sidestep the issue of possible pollutants contaminating the fertilizer products. Future studies need to be conducted to better understand the rejection of pharmaceuticals by AEMspharmaceutical.

An alternative method to circumvent both the sodium and product contamination issues is to recover the orthophosphates in DD receiver solutions with little or no Na^+. In this approach, initial receiver solutions that contain sufficiently high concentrations of Cl^- but with cations other than Na^+ are used. Additionally, the cations can be K^+ and NH_4^+ to further valorize nutrient content of the fertilizer product. For instance, aqueous solutions of potash fertilizer, $KCl_{(aq)}$, can be used

as the RS (simulated as 600 $\times 10^{-3}$ mol/L KCl here), to draw additional value through the exchange of orthophosphate and Cl^-. Another RS option is waste water softening regenerant rinse (WWSRR), which contains a high concentration of chloride anions and potassium and magnesium as the cations (approximately 547×10^{-3} mol/L K^+, 48×10^{-3} mol/L Mg^{2+}, and 643×10^{-3} mol/L Cl^-). Diluted bittern (DB), a concentrated byproduct of table salt production from seawater, is yet another alternative. DB contains approximately 77 $\times 10^{-3}$ mol/L K^+, 252×10^{-3} mol/L Mg^{2+}, 25×10^{-3} mol/L SO_4^{2-}, 8×10^{-3} mol/L NH_4^+, 615×10^{-3} mol/L Cl^-, and 26×10^{-3} mol/L Na^+. Note that the concentration of Na^+ in diluted bittern is sufficiently low and can be tolerated by some plant species, such as beets (Kronzucker et al., 2013; Lawlor and Milford, 1973). DD experiments were conducted using simulated aqueous potash solutions (APS), WWSRR, and DB, with the ASVN membrane, simulated fresh urine as FS, and V_{FS}/V_{RS} of 1. Figure 8 presents fluxes of $H_xPO_4^{(3-x)-}$ and SO_4^{2-} from FS to RS.

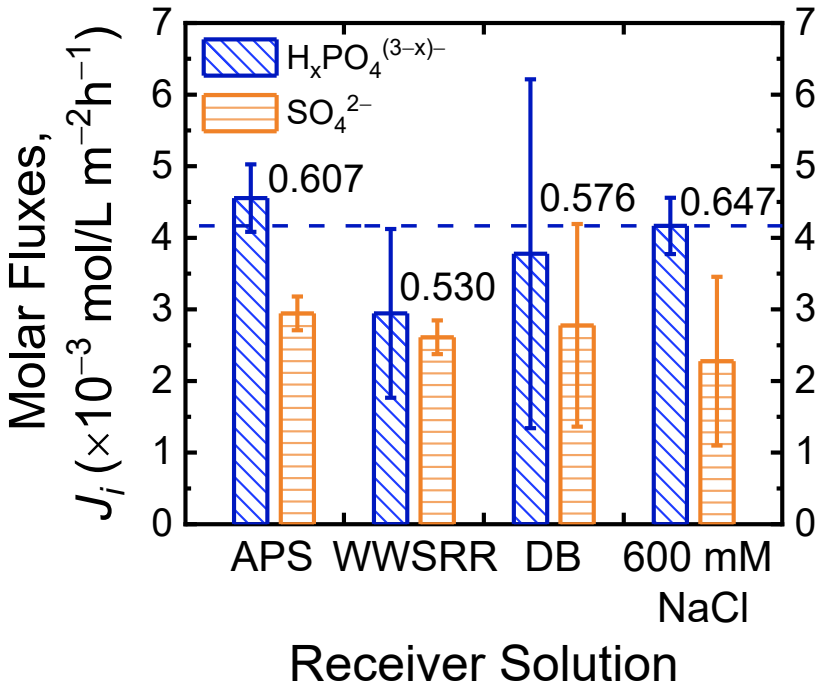

705

706 **Figure 8.** Fluxes of $H_xPO_4^{(3-x)-}$ and SO_4^{2-} (blue and orange columns, respectively) in kinetic
707 experiments with different initial receiver solutions of simulated aqueous potash solution (APS, $[Cl^-]$ =
708 600×10^{-3} mol/L), simulated waste water softening regenerant rinse, (WWSRR, $[Cl^-] = 643\times10^{-3}$ mol/L),
709 and simulated diluted bittern (DB, $[Cl^-] = 615\times10^{-3}$ mol/L). Fluxes with RS of 600×10^{-3} mol/L NaCl
710 are included for comparison. For all experiments simulated fresh urine was used as the FS and V_{FS}/V_{RS}
711 = 1. Labels above the $H_xPO_4^{(3-x)-}$ columns denote the selectivity for orthophosphate, J_P/J_T. Horizontal
712 line is orthophosphate flux in DD with 600×10^{-3} mol/L NaCl. All experiments utilized ASVN
713 membranes. Data points and error bars are means and standard deviations, respectively, of duplicate
714 experiments.

715 In general, J_P (and J_S) of the different simulated receiver solutions are comparable with the
716 600×10^{-3} mol/L NaCl RS. Similar J_P are expected because all operations utilized the same FS and
717 have fairly similar $[Cl^-]_{RS,0}$ (< 7% difference). Importantly, DD with the monovalent ion selective
718 membrane (ASVN) consistently achieved selectivity for $H_xPO_4^{(3-x)-}$ flux over SO_4^{2-} for all the
719 simulated receiver solutions (J_P/J_T = 0.53–0.61). This highlights the flexibility of DD to utilize

different Cl^--rich streams, including waste and low-cost sources, as the receiver solution for orthophosphate recovery from fresh urine. Additionally, the RS can be rationally selected to promote mineral precipitation, to enable recovery of solid orthophosphates. For instance, precipitated phosphate salts of calcium and magnesium can be further isolated from the liquid stream when Ca^{2+}- and Mg^{2+}-rich WWSRR is used as the RS.

5. Implications

The current P management practices are unsustainable. Phosphate is mined and processed from diminishing reserves at immense energy costs. P-rich excretions are heavily diluted in the traditional wastewater system, which contributes to the high energy and chemical expenditures in efforts to remove the phosphates from wastewaters. When not adequately removed, P is released into the environment, causing ecological harm and public health concerns. Further compounding to these issues are environmental problems associated with phosphate fertilizer manufacturing, in particular, the radioactive byproducts that are generated. Improper storage and management of the radioactive wastes pose leakage risks (Nelson et al., 2021; Sandhu et al., 2018). These hazards were starkly exposed in March 2021 when the Piney Point, Florida, production plant leaked radioactive phosphogypsum into Tampa Bay because of an engineering failure in the aged infrastructure. Residents of the surrounding area were evacuated due to risks of contact with the contaminated waters (Nelson et al., 2021). The inefficient linear economy approach and this unfortunate incident underscore the need for a paradigm shift to a circular P economy with sustainable phosphate capture and reuse.

The high concentrations of orthophosphate anion in human urine offer propitious opportunities for recovery. Donnan dialysis can utilize driver ions to exchange for $H_xPO_4^{(3-x)-}$ in

742 the urine feed, capturing P in the receiver solution for application as fertilizer. This study
743 demonstrates that Donnan dialysis can i) recover orthophosphate from urine, ii) enrich
744 orthophosphate in the receiver solution, iii) selectively capture orthophosphate over other anions
745 by utilizing fresh urine and monovalent ion permselective membranes, and iv) leverage on widely
746 available and low-cost/waste resources to drive orthophosphate recovery. Importantly, using
747 receiver streams with adequately high driver ion concentrations in DD (Cl^- in this study) can
748 enable orthophosphate transport against a concentration gradient and attain "uphill transport" to
749 reach practically feasible recovery yields (> 80% demonstrated in this investigation). By
750 employing a smaller receiver solution volume relative to the feed, DD can achieve enrichment of
751 orthophosphate, i.e., P concentration in the product is higher than in fresh urine. A fertilizer product
752 with high orthophosphate concentrations is of greater economic value and additionally facilitates
753 transportation. The analysis also reveals the rationale for using fresh, rather than hydrolyzed urine,
754 for P recovery. Specifically, the high bicarbonate content of the latter source is detrimental to
755 orthophosphate flux and selectivity. This indicates that DD orthophosphate recovery should be
756 performed immediately after urine diversion and collection, prior to urea hydrolysis. Alternatively,
757 dosing with inhibitory compounds, electrochemical treatment, or acid/base addition can inactivate
758 the urease enzyme, (Hellström et al., 1999; Ikematsu et al., 2007; Lv et al., 2020; Randall et al.,
759 2016; Saettaab et al., 2020; Svane et al., 2020; Udert et al., 2003a; Udert et al., 2003b) thus
760 suppressing bicarbonate formation.

761 Besides bicarbonate, sulfate can compete with orthophosphate anions to exchange with
762 driver chloride ions, hence reducing recovery efficiency. The study highlights the applicability of
763 using monovalent ion permselective membrane to drive more selective transport of orthophosphate
764 over sulfate. However, the improvements in selectivity are at the cost of decreased kinetics.

765 Therefore, the overall DD process would need to simultaneously consider TOP recovery yields
766 and membrane requirements, i.e., tradeoffs between with economic benefits with capital and
767 operating costs. Thoughtful selection of the receiver stream offers flexibility in tailoring the water
768 chemistry and nutrient profile of the fertilizer product. Critically, economic viability of P recovery
769 with DD can be enhanced by utilizing waste/low-cost streams as the receiver solution. For example,
770 waste water softening regenerant rinse generated in residential buildings can be repurposed to
771 supply the high chloride concentrated needed in the receiver solution, to drive DD recovery of
772 orthophosphate from diverted urine from the same premises. Future investigations will be needed
773 to understand the potential impacts of other compounds in urine, such as pharmaceuticals,
774 pathogens, and other contaminants, on DD performance and phosphate recovery (including
775 membrane fouling).

776 The insights from this study are broadly applicable to other DD processes for resource
777 recovery or contaminant removal, particularly for streams with multiple anions and/or cations.
778 Some examples are NH_4^+ recovery from wastewater, metal ion recovery from electroplating rinse,
779 and removal of NO_3^- and $H_xAsO_4^{(3-x)-}$ from drinking water. The approach for determining ion
780 concentrations in feed and receiver solutions at Donnan equilibrium presented here (eqs S9–13)
781 can be utilized to project target ion recovery potential or contaminant removal efficiency from
782 mixed electrolyte solutions. Furthermore, the systematic analysis of factors influencing fluxes of
783 different ions underscores the role of competitive ion sorption on transport kinetics and can
784 elucidate ion transport behavior in solutions with complex compositions. In applications where
785 multivalent species are present together with the monovalent target ion, as in NH_4^+ recovery from
786 wastewater or NO_3^- removal from drinking water, MIPMs may be useful to improve selectivity
787 for the target species with an acceptable sacrifice in permeation flux.

Acknowledgements

This material is based upon work supported by the National Science Foundation under Grant No. 1903705 and the Science Pathways Scholars Program of Barnard College. Any opinions, findings, and conclusions or recommendations expressed in this material are those of the author(s) and do not necessarily reflect the views of the National Science Foundation or Barnard College.

References

2002 ITP Mining: Energy and Environmental Profile of the U.S. Mining Industry Department of Energy, Office of Energy Efficiency & Renewable Energy.

Anderson, D.M., Burkholder, J.M., Cochlan, W.P., Glibert, P.M., Gobler, C.J., Heil, C.A., Kudela, R., Parsons, M.L., Rensel, J.E., Townsend, D.W., Trainer, V.L. and Vargo, G.A. 2008. Harmful algal blooms and eutrophication: Examining linkages from selected coastal regions of the United States. Harmful Algae 8(1), 39-53.

Arola, K., Ward, A., Mänttäri, M., Kallioinen, M. and Batstone, D. 2019. Transport of pharmaceuticals during electrodialysis treatment of wastewater. Water Res 161, 496-504.

Asante-Sackey, D., Rathilal, S., Tetteh, E.K., Ezugbe, E.O. and Pillay, L.V. 2021. Donnan Membrane Process for the Selective Recovery and Removal of Target Metal Ions—A Mini Review. Membranes 11(358).

Banasiaka, L.J., Bruggen, B.V.d. and Schäfer, A.I. 2011. Sorption of pesticide endosulfan by electrodialysis membranes. Chem Eng J 116(1), 233-239.

Beck, A. and Ernst, M. 2015. Kinetic modeling and selectivity of anion exchange in Donnan dialysis. J. Membr. Sci. 479, 132-140.

Blackall, L.L., Crocetti, G.R., Saunders, A.M. and Bond, P.L. 2002. A review and update of the microbiology of enhanced biological phosphorus removal in wastewater treatment plants. Antonie Van Leeuwenhoek 81(1-4), 681-691.

Bleiwas, D.I. 2011 Estimates of Electricity Requirements for the Recovery of Mineral Commodities, with Examples Applied to Sub-Saharan Africa, Reston, VA.

Boer, M.A.d., Hammerton, M. and Slootweg, J.C. 2018. Uptake of pharmaceuticals by sorbent-amended struvite fertilisers recovered from human urine and their bioaccumulation in tomato fruit. Water Res 133, 19-26.

Brooks, B.W., Lazorchak, J.M., Howard, M.D.A., Johnson, M.V.V., Morton, S.L., Perkins, D.A.K., Reavie, E.D., Scott, G.I., Smith, S.A. and Steevens, J.A. 2016. Are Harmful Algal Blooms Becoming the Greatest Inland Water Quality Threat to Public Health and Aquatic Ecosystems? Environ. Toxicol. Chem. 35(1), 6-13.

821 Chen, S.Y., Shi, Z., Song, Y., Li, X.R. and Hu, Y.L. 2014. Phosphate removal from aqueous
822 solution by Donnan dialysis with anion-exchange membrane. J Cent South Univ 21(5),
823 1968-1973.

824 Commoner, B. (1971) The Closing Circle: Nature, Man, and Technology, Random House, New
825 York.

826 Conley, D.J., Paerl, H.W., Howarth, R.W., Boesch, D.F., Seitzinger, S.P., Havens, K.E., Lancelot,
827 C. and Likens, G.E. 2009. Ecology - Controlling eutrophication: Nitrogen and phosphorus.
828 Science 323, 1014-1015.

829 Diaz, R.J. and Rosenberg, R. 2008. Spreading dead zones and consequences for marine
830 ecosystems. Science 321, 926-929.

831 Elser, J. and Bennett, E. 2011. A broken biogeochemical cycle. Nature 478(7367), 29-31.

832 Fan, H., Huang, Y., Billinge, I.H., Bannon, S.M., Geise, G.M. and Yip, N.Y. 2022. Counterion
833 Mobility in Ion-Exchange Membranes: Spatial Effect and Valency-Dependent
834 Electrostatic Interaction. ACS EST Engg.

835 Fittschen, I. and Hahn, H.H. 1998. Characterization of the municipal wastewaterpart human urine
836 and a preliminary comparison with liquid cattle excretion. Water Sci. Technol. 38(6), 9-16.

837 Galizia, M., Benedetti, F.M., Paula, D.R. and Freeman, B.D. 2017. Monovalent and divalent ion
838 sorption in a cation exchange membrane based on cross-linked poly (p-styrene sulfonate-
839 co-divinylbenzene). J. Membr. Sci. 525, 132-142.

840 Genc, Y., McDonald, G.K. and Tester, M. 2007. Reassessment of tissue Na+ concentration as a
841 criterion for salinity tolerance in bread wheat. Plant Cell Environ 30, 1-23.

842 Guest, J.S., Skerlos, S.J., Barnard, J.L., Beck, M.B., Daigger, G.T., Hilger, H., Jackson, S.J.,
843 Karvazy, K., Kelly, L., Macpherson, L., Mihelcic, J.R., Pramanik, A., Raskin, L., Van
844 Loosdrecht, M.C.M., Yeh, D. and Love, N.G. 2009. A new planning and design paradigm
845 to achieve sustainable resource recovery from wastewater. Environ. Sci. Technol.

846 H. Jönsson, B.V. 2004 Adapting the nutrient content of urine and faeces in different countries
847 using FAO and Swedish data, pp. 7-11.

848 Hellström, D., Johannson, E. and Grennberg, K. 1999. Storage of human urine: acidification as a
849 method to inhibit decomposition of urea. Ecol. Eng. 12(3-4), 253-269.

850 Hichour, M., Persin, F., Sandeaux, J. and Gavach, C. 2000. Fluoride removal from waters by
851 Donnan dialysis. Separation and Purification Technology 18(1), 1-11.

852 Hitzfeld, B.C., Hoger, S.J. and Dietrich, D.R. 2000. Cyanobacterial toxins: Removal during
853 drinking water treatment, and human risk assessment. Environ Health Persp 108, 113-122.

854 Ikematsu, M., Kaneda, K., Iseki, M. and Yasuda, M. 2007. Electrochemical treatment of human
855 urine for its storage and reuse as flush water. Sci. Total Environ. 382(1), 159-164.

856 J. Veermana, J., de Jong, R.M., M., S., Metz, S.J. and Harmsen, G.J. 2009. Reverse electrodialysis:
857 Comparison of six commercial membrane pairs on the thermodynamic efficiency and
858 power density. y. J. Membr. Sci. 2 343(1-2), 7-15.

Karageorgiou, K., Paschalis, M. and Anastassakis, G.N. 2007. Removal of phosphate species from solution by adsorption onto calcite used as natural adsorbent. Journal of Hazardous Materials 139(3), 447-452.

Karak, T. and Bhattacharyya, P. 2011. Human urine as a source of alternative natural fertilizer in agriculture: A flight of fancy or an achievable reality. Resour Conserv Recy 55(4), 400-408.

Kemacheevakul, P., Chuangchote, S., Otani, S., Matsuda, T. and Shimizu, Y. 2015. Effect of magnesium dose on amount of pharmaceuticals in struvite recovered from urine. Water Sci. Technol. 72(7), 1102-1110.

Kronzucker, H.J., Coskun, D., Schulze, L.M., Wong, J.R. and Britto, D.T. 2013. Sodium as nutrient and toxicant. Plant Soil 369, 1-23.

Lahr, R.H., Goetsch, H.E., Haig, S.J., Noe-Hays, A., Love, N.G., Aga, D.S., Bott, C.B., Foxman, B., Jimenez, J., Luo, T., Nace, K., Ramadugu, K. and Wigginton, K.R. 2016. Urine Bacterial Community Convergence through Fertilizer Production: Storage, Pasteurization, and Struvite Precipitation. Environ. Sci. Technol. 50, 11619−11626.

Larsen, T.A., Alder, A.C., Eggen, R.I.L., Maurer, M. and Lienert, J. 2009. Source separation: Will we see a paradigm shift in wastewater handling? Environ. Sci. Technol. 43(16), 6121.

Larsen, T.A., Maurer, M., Udert, K.M. and Lienert, J. 2007. Nutrient cycles and resource management: implications for the choice of wastewater treatment technology. Water Sci. Technol. 56(5), 229-237.

Larsen, T.A., Udert, K.M. and Lienert, J. (2013) Source separation and decentralization for wastewater management, Iwa Publishing.

Lawlor, D.W. and Milford, G.F.J. 1973. The effect of sodium on growth of water-stressed sugar-beet. Ann. Bot. 37(3), 597–604.

Li, W.W., Yu, H.Q. and Rittmann, B.E. 2015. Chemistry: Reuse water pollutants. Nature 528(7580), 29-31.

Liu, Y., Kumar, S., Kwag, J.H. and Ra, C. 2013. Magnesium ammonium phosphate formation, recovery and its application as valuable resources: a review. J Chem Technol Biot 88(2), 181-189.

Lu, H.-Y., Lin, C.-S., Lee, S.-C., Ku, M.-H., Hsu, J.-P., Tseng, S. and Lin, S.-H. 2011. Preparation of Mineral Source Water From Deep Sea Water: Reduction of Sulfate Ion Using Selemion ASV Membrane. AIChE Journal 5(4), 1033-1042.

Lu, J.B., Liu, H.J., Liu, R.P., Zhao, X., Sun, L.P. and Qu, J.H. 2013. Adsorptive removal of phosphate by a nanostructured Fe-Al-Mn trimetal oxide adsorbent. Powder Technol 233, 146-154.

Lv, Y., Li, Z., Zhou, X., Cheng, S. and Zheng, L. 2020. Stabilization of source-separated urine by heat-activated peroxydisulfate. Sci. Total Environ. 749.

Ma, L., Gutierrez, L., Verbeke, R., D'Haese, A., Waqas, M., Dickmann, M., Helm, R., Vankelecom, I., Verliefde, A. and Cornelissen, E. 2021a. Transport of organic solutes in ion-exchange

membranes: Mechanisms and influence of solvent ionic composition. Water Res 190, 116756.

Ma, L., Gutierrez, L., Vooren, T.V., Vanoppen, M., Kazemabad, M., Verliefde, A. and Cornelissen, E. 2021b. Fate of organic micropollutants in reverse electrodialysis: Influence of membrane fouling and channel clogging. Desalination 512, 115114.

Malewitz, T., Pintauro, P.N. and Rear, D. 2007. Multicomponent absorption of anions in commercial anion-exchange membranes. J. Membr. Sci. 301, 171-179.

Maul, G.A., Kim, Y., Amini, A., Zhang, Q. and Boyer, T.H. 2014. Efficiency and life cycle environmental impacts of ion-exchange regeneration using sodium, potassium, chloride, and bicarbonate salts. Chem Eng J 254, 198-209.

Maurer, M., Pronk, W. and Larsen, T.A. 2006. Treatment processes for source-separated urine. Water Res. 40(17), 3151-3166.

Maurer, M., Schwegler, P. and Larsen, T.A. 2003. Nutrients in urine: energetic aspects of removal and recovery. Water Sci. Technol. 48(1), 37-46.

McCartney, S.N., Watanabe, N.S. and Yip, N.Y. 2021. Thermodynamic and energy analysis of nitrogen and phosphorous recovery from wastewaters. Environ. Sci.: Water Res. Technol. 7(11), 2075-2088.

McCartney, S.N., Williams, N., Boo, C., Chen, X. and Yip, N.Y. 2020. Novel Isothermal Membrane Distillation with Acidic Collector for Selective and Energy-Efficient Recovery of Ammonia from Urine. ACS Sustain. Chem. Eng. 8(19), 7324–7334.

Michalak, A.M., Anderson, E.J., Beletsky, D., Boland, S., Bosch, N.S., Bridgeman, T.B., Chaffin, J.D., Cho, K., Confesor, R., Daloglu, I., DePinto, J.V., Evans, M.A., Fahnenstiel, G.L., He, L., Ho, J.C., Jenkins, L., Johengen, T.H., Kuo, K.C., LaPorte, E., Liu, X., McWilliams, M.R., Moore, M.R., Posselt, D.J., Richards, R.P., Scavia, D., Steiner, A.L., Verhamme, E., Wright, D.M. and Zagorski, M.A. 2013. Record-setting algal bloom in Lake Erie caused by agricultural and meteorological trends consistent with expected future conditions. Proc. Natl. Acad. Sci. 110(16), 6448-6452.

Mihelcic, J.R., Fry, L.M. and Shaw, R. 2011. Global potential of phosphorus recovery from human urine and feces. Chemosphere 84(6), 832-839.

Mogollóna, J.M., Beusenab, A.H.W., H.J.Mvan Grinsvenb, H.J., Westhoekb, H. and Bouwmanab, A.F. 2018. Future agricultural phosphorus demand according to the shared socioeconomic pathways. Glob. Environ. Change 50, 149-163.

Mullen, R.A., Wigginton, K.R., Noe-Hays, A., Nace, K., Love, N.G., Bottd, C.B. and Aga, D.S. 2017. Optimizing extraction and analysis of pharmaceuticals in human urine, struvite, food crops, soil, and lysimeter water by liquid chromatography-tandem mass spectrometry. Anal. Methods 9.

Nelson, N.G., Cuchiara, M.L., Hendren, C.O., Jones, J.L. and Marshall, A.-M. 2021. Hazardous Spills at Retired Fertilizer Manufacturing Plants Will Continue to Occur in the Absence of Scientific Innovation and Regulatory Enforcement. Environ. Sci. Technol. 55(24), 16267–16269.

Oehmen, A., Lemos, P.C., Carvalho, G., Yuan, Z., Keller, J., Blackall, L.L. and Reis, M.A. 2007. Advances in enhanced biological phosphorus removal: from micro to macro scale. Water Res. 41(11), 2271-2300.

Pessoa-Lopes, M., Crespo, J.G. and Velizarov, S. 2016. Arsenate removal from sulphate-containing water streams by an ion-exchange membrane process. Sep. Purif. Technol. 166, 125-134.

Pronk, W., Biebow, M. and Boller, M. 2006. Electrodialysis for Recovering Salts from a Urine Solution Containing Micropollutants. Environ. Sci. Technol. 40(7), 2414–2420.

Rahman, M.M., Salleh, M.A.M., Rashid, U., Ahsan, A., Hossain, M.M. and Ra, C.S. 2014. Production of slow release crystal fertilizer from wastewaters through struvite crystallization - A review. Arab. J. Chem. 7(1), 139-155.

Randall, D.G., Krähenbühl, M., Köpping, I., Larsen, T.A. and Udert, K.M. 2016. A novel approach for stabilizing fresh urine by calcium hydroxide addition. Water Res 95, 361-369.

Randall, D.G. and Naidoo, V. 2018. Urine: The liquid gold of wastewater. J. Environ. Chem. Eng. 6(2), 2627-2635.

Reta, G., Dong, X., Li, Z., Su, B., Hu, X., Bo, H., Yu, D., Wan, H., Liu, J., Li, Y., Xu, G., Wang, K. and Xu, S. 2018. Environmental impact of phosphate mining and beneficiation: review. Int. J. Hydrol. Sci. 2(4), 424-431.

Ronteltap, M., Maurer, M. and Gujer, W. 2007a. The behaviour of pharmaceuticals and heavy metals during struvite precipitation in urine. Water Res 41(9), 1859-1868.

Ronteltap, M., Maurer, M. and Gujer, W. 2007b. Struvite precipitation thermodynamics in source-separated urine. Water Res. 41(5), 977-984.

Saettaab, D., Zhengab, C., Leyvaac, C. and Boyer, T.H. 2020. Impact of acetic acid addition on nitrogen speciation and bacterial communities during urine collection and storage. Sci. Total Environ. 745.

Sandhu, D., Singh, A., Duranceau, S.J., Nam, B.H., Mayo, T. and Wang, D. 2018. Fate and transport of radioactive gypsum stack water entering the Floridan aquifer due to a sinkhole collapse. Sci. Rep. 8.

Saracco, G. 1997. Transport properties of monovalent-ion-permselective membranes. Chem. Eng. Sci. 52(17), 3019-3031.

Saracco, G. and Zanetti, M.C. 1994. Ion transport through monovalent-anion-permselective membranes. Ind Eng Chem Res 33(1), 96-101.

Sarkar, S., Sengupta, A.K. and Prakash, P. 2010. The Donnan Membrane Principle: Opportunities for Sustainable Engineered Processes and Materials. Environ. Sci. Technol. 44(4), 1161-1166.

Schaubroeck, T., De Clippeleir, H., Weissenbacher, N., Dewulf, J., Boeckx, P., Vlaeminck, S.E. and Wett, B. 2015. Environmental sustainability of an energy self-sufficient sewage treatment plant: Improvements through DEMON and co-digestion. Water Res. 74, 166-179.

977 Shashvatt, U., Amurrio, F., Portner, C. and Blaney, L. 2021. Phosphorus recovery by Donnan
978 dialysis: Membrane selectivity, diffusion coefficients, and speciation effects. Chem. Eng.
979 J. 419.

980 Simha, P. and Ganesapillai, M. 2017. Ecological Sanitation and nutrient recovery from human
981 urine: How far have we come? A review. Sustain. Environ. Res 27(3), 107-116.

982 Smil, V. 2000. Phosphorus in the Environment: Natural Flows and Human Interferences. Annu.
983 Rev. Environ. Resour. 25, 53-88.

984 Spiegler, K.S. 1958. Transport processes in ionic membranes. Trans. Faraday Soc. 54, 1408-1428.

985 Stahel, W.R. 2016. The circular economy. Nature 531(7595), 435-438.

986 Steffen, W., Richardson, K., Rockstrom, J., Cornell, S.E., Fetzer, I., Bennett, E.M., Biggs, R.,
987 Carpenter, S.R., de Vries, W., de Wit, C.A., Folke, C., Gerten, D., Heinke, J., Mace, G.M.,
988 Persson, L.M., Ramanathan, V., Reyers, B. and Sorlin, S. 2015. Planetary boundaries:
989 Guiding human development on a changing planet. Science 347(6223).

990 Strathmann, H. (1995) Membrane Science and Technology. Noble, R.D. and Stern, S.A. (eds), pp.
991 213-281, Elsevier.

992 Strathmann, H. (2004) Ion-Exchange Membrane Separation Processes, Elsevier.

993 Strathmann, H. 2010. Ion-Exchange Membrane Processes in Water Treatment. Sustainable Water
994 for the Future: Water Recycling Versus Desalination 2, 141-199.

995 Svane, S., Sigurdarson, J.J., Finkenwirth, F., Eitinger, T. and Karring, H. 2020. Inhibition of
996 urease activity by different compounds provides insight into the modulation and
997 association of bacterial nickel import and ureolysis. Sci. Rep. 10.

998 Tanada, S., Kabayama, M., Kawasaki, N., Sakiyama, T., Nakamura, T., Araki, M. and Tamura, T.
999 2003. Removal of phosphate by aluminum oxide hydroxide. J Colloid Interf Sci 257(1),
1000 135-140.

1001 Tanaka, Y. (2015) Ion Exchange Membranes: Fundamentals and Applications, pp. 445-457, IEM
1002 Research, Ibaraki, Japan.

1003 Tang, C., Liua, Z., Penga, C., Chaia, L.-Y., Kurodac, K., Okidoc, M. and Song, Y.-X. 2019. New
1004 insights into the interaction between heavy metals and struvite: Struvite as platform for
1005 heterogeneous nucleation of heavy metal hydroxide. Chem Eng J 365, 60-69.

1006 Trifi, I.M., Trifi, B., Ayed, S.B. and Hamrouni, B. 2009. Removal of phosphate by Donnan
1007 dialysis coupled with adsorption onto calcium alginate beads. Water Sci. Technol. 80(1).

1008 Udert, K.M., Larsen, T.A., Biebow, M. and Gujer, W. 2003a. Urea hydrolysis and precipitation
1009 dynamics in a urine-collecting system. Water Res. 37(11), 2571-2582.

1010 Udert, K.M., Larsen, T.A. and Gujer, W. 2003b. Estimating the precipitation potential in urine-
1011 collecting systems. Water Res. 37(11), 2667-2677.

1012 Vanoppen, M., Bakelants, A.F.A.M., Gaublomme, D., Schoutteten, K.V.K.M., Bussche, J.V.,
1013 Vanhaecke, L. and Verliefde, A.R.D. 2015. Properties Governing the Transport of Trace
1014 Organic Contaminants through Ion-Exchange Membranes. Environ. Sci. Technol. 49(1),
1015 489–497.

1016 Velizarov, S. 2013. Transport of arsenate through anion-exchange membranes in Donnan dialysis.
1017 J. Membr. Sci. 425, 243-250.

1018 Verstraete, W., de Caveye, P.V. and Diamantis, V. 2009. Maximum use of resources present in
1019 domestic "used water". Bioresour. Technol. 100(23), 5537-5545.

1020 W. McDonough, M.B. (2002) Cradle to Cradle: Remaking the Way We Make Things, North Point
1021 Press, New York.

1022 Wang, J., Burken, J.G., Zhang, X.Q. and Surampalli, R. 2005. Engineered struvite precipitation:
1023 Impacts of component-ion molar ratios and pH. J Environ Eng 131(10), 1433-1440.

1024 Webster, K. (2015) The Circular Economy: a Wealth of Flows, Ellen MacArthur Foundation, Isle
1025 of Wight.

1026 Xie, J., Wang, Z., Lu, S.Y., Wu, D.Y., Zhang, Z.J. and Kong, H.N. 2014. Removal and recovery
1027 of phosphate from water by lanthanum hydroxide materials. Chem Eng J 254, 163-170.

1028 Yan, G.J., Bao, Y., Tan, M., Cui, Q., Lu, X.L. and Zhang, Y. 2018. Defluorination by Donnan
1029 Dialysis with seawater for seafood processing. J Food Eng 238, 22-29.

1030 Yeoman, S., Stephenson, T., Lester, J.N. and Perry, R. 1988. The removal of phosphorus during
1031 wastewater treatment: a review. Environ. Pollut. 49(3), 183-233.

1032 Yip, N.Y. and Elimelech, M. 2012. Thermodynamic and energy efficiency analysis of power
1033 generation from natural salinity gradients by pressure retarded osmosis. Environ. Sci.
1034 Technol. 46(9), 5230-5239.

1035 Zhang, G.S., Liu, H.J., Liu, R.P. and Qu, J.H. 2009. Removal of phosphate from water by a Fe-
1036 Mn binary oxide adsorbent. J. Colloid Interface Sci. 335(2), 168-174.

1037 Zhao, B., Zhao, H. and Ni, J. 2010. Arsenate removal by Donnan dialysis: Effects of the
1038 accompanying components. Sep. Purif. Technol. 72(3), 250-255.